Partial Phenotyping of an Idiopathic Infantile Hypercalcemia Mouse Model

Dila Kavame, MD

Department of Human Genetics
Faculty of Medicine and Health Sciences
McGill University, Montréal, Québec, Canada

March 2022

A thesis submitted to McGill University in partial fulfillment of the requirements of the degree of Master of Science in Human Genetics.

Abstract

Vitamin D is fundamental to mineral homeostasis, and bone development. Disorders in vitamin D metabolism lead to pathologies. For example, loss-of-function mutations in the *CYP24A1* gene were discovered as the first underlying genetic defects in Idiopathic Infantile Hypercalcemia (IIH). Recently, it has been reported that the R396W mutation in the *CYP24A1* gene is detected at high frequency in IIH patients. Our team previously showed that *Cyp24a1*-null mice with a deletion of exons 9-10, unable to produce $24,25(OH)_2D_3$, mimicked the disease IIH. The mice also displayed impaired callus formation during the endochondral phase of fracture repair. Based on this earlier work, we hypothesized that a humanized mouse model sporting the site-specific R396W mutation will also exhibit impaired fracture repair.

We commercially contracted out the R396W knock-in embryonic stem (ES) cells and generated R396W-CD1 mouse strain which is a valid mimic of the IIH human condition. We then performed rodded tibial osteotomy on wild-type, heterozygous and homozygous R396W mutated mice. We harvested healing bones at intervals and tested their biomechanical properties.

Despite experimental challenges, torsion tests showed decreased stiffness of the healing calluses in mutant animals. Micro-Computed Tomography (µCT) scanning, and 3-Point Bending Tests (3PBT) showed significant differences in load at break (strength) in both male and female mutants compared to heterozygous and/or wild-type littermates.

Our results indicate that the humanized preclinical model of IIH, R396W-CD1 strain, has similar phenotypic manifestations to the original *Cyp24a1*-null mice. Furthermore, we suggested that $24,25(OH)_2D_3$ has an earlier effect during fracture repair than previously evaluated.

Résumé

La vitamine D est essentielle à l'homéostasie minérale et au développement osseux. Des troubles du métabolisme de la vitamine D entraînent des pathologies. Par exemple, des mutations de perte de fonction dans le gène *CYP24A1* ont été découvertes comme les premiers défauts génétiques sous-jacents dans l'hypercalcémie infantile idiopathique (IIH). Il a été rapporté que la mutation R396W du gène *CYP24A1* est détectée à haute fréquence chez les patients IIH. Notre équipe a précédemment montré que des souris mutantes pour *Cyp24a1* avec une délétion des exons 9-10 présentent un phénotype comparable à IIH. Les souris montrent aussi une formation de cals altérée pendant la phase endochondrale de la réparation des fractures. Sur la base de ces travaux antérieurs, nous avons émis l'hypothèse qu'un modèle de souris humanisé portant la mutation ciblée R396W présentera également une réparation de fracture altérée.

Nous avons généré la souche de souris R396W-CD1 qui est une phénocopie valide de la condition humaine IIH. Nous avons ensuite réalisé une ostéotomie tibiale immobilisée par tige sur des souris sauvages, hétérozygotes et homozygotes R396W. Nous avons prélevé les os en cours de guérison à intervalles réguliers et testé leurs propriétés biomécaniques.

Malgré des défis expérimentaux, les tests de torsion ont montré une diminution de la rigidité des cals cicatrisants chez les animaux mutants. La tomographie assistée par ordinateur (µCT) et les tests de flexion en 3 points (3PBT) ont montré des différences significatives de charge à la rupture (force) chez les mutants mâles et femelles par rapport aux compagnons de litière hétérozygotes et/ou de type sauvage.

Nos résultats indiquent que le modèle préclinique humanisé de l'IIH, la souche R396W-CD1, présente des manifestations phénotypiques similaires à celles des souris originales

Cyp24a1-null. De plus, nous avons suggéré que le 24,25$(OH)_2D_3$ a un effet plus précoce lors de la réparation des fractures que précédemment évalué.

Table of Contents

List of Abbreviations

List of Figures

Acknowledgements

I remember how this work started as an idea and evolved throughout the project. Science gives you the opportunity to see the ideas come to reality, and this is what makes it special. It was not always an easy journey but being surrounded by supportive people makes it an enjoyable one.

First and foremost, I would like to begin to express my sincere gratitude to my supervisor, Dr. René St-Arnaud, for taking me under his supervision. It was a great opportunity to be part of his scientific team. Without his guidance, support, and patience none of this would have been possible. I remember he was saying that “The day that you learn something, you don’t die”. His hunger for learning inspired me during this hard work and the very new field of mine.

I want to express my sincere thanks to my supervisory committee members: Dr. Monzur Murshed and Dr. Pierre Moffatt. Your critical thinking, authentic approach, and experimental ability gave me the encouragement I needed to advance my scientific knowledge.

A tremendous thank you to my colleague and friend, Dr. Hadla Hariri. Her support kept me motivated. She is a great teacher, a true mentor, and a lovable friend I could have asked for. And big thanks to my past and present coworkers Dr. Alice Arabian, Dr. Martin Pelicelli, Dr. Priscilla Doyon, Dr. Omar Al-Rifai, and Dr. Mahmoud Ismail. Their positive and friendly attitude is exceptional and being surrounded by them was a big luck to me.

Of course, I have enormous gratitude and love for my family and friends. Their immense support from all around the world was precious to me. Loads of love go to my dearest friends Bengisu Ozarslan, Burak Ozer, Makbule Gizem Cayirli, Dilek Sarikaya, Nimet Tugce Parlar, and Yasmeen Hitti for their precious friendship. And a special thanks to Paul-Louis Crouzat, for being there when I needed it the most.

Finally, my family Zehra Kavame, Cenk Kavame, and my dearest grandmother, Gazve Kavame. All I can say is that I thank you for everything you have given me in my life.

Format of the Thesis

The thesis is written and submitted in the traditional format. It contains a total of six chapters and appendix.

Chapter 1 comprises of the introduction. Here we give an overview of key features in bone physiology. We cover bone development, mineralisation and chondrocyte differentiation, bone as an endocrine organ, fracture repair stages, vitamin D metabolism, CYP24A1 and $24,25(OH)_2D_3$, Idiopathic Infantile Hypercalcemia and *Cyp24a1*-null mice.

Chapter 2 is the materials and methods section. Here we lay out the methodology, experiments and tools utilized in our study.

Chapter 3 is the result section. Here we present all the findings of our study.

Chapter 4 consists of the discussion section. We summarize our work in the context of previously published literature and provide some limitations of our study.

Chapter 5 concludes the thesis with a description of possible future directions. We present methodologies that can be used to further analyze the implications of our findings.

Chapter 6 catalogues our references.

And **Appendix** includes the copyrights and permissions of the figures that been used in the thesis and finally the research ethic board approval for mice studies.

Contribution of Authors

Dr. Dila Kavame and Dr. René St-Arnaud were responsible for designing the study. The torsion test technique was developed by Dila Kavame under the supervision of Dr. René St-Arnaud. All data generated in this study was obtained by Dila Kavame. Dila Kavame and Dr. René St-Arnaud performed the relevant data analysis. Result interpretation was completed by Dila Kavame and Dr. René St-Arnaud. Funding for this study was obtained by Dr. René St-Arnaud. Initial thesis draft was completed by Dila Kavame. Editing and approval of final version of the thesis was completed by Dr. René St-Arnaud.

Chapter I: Introduction, Hypothesis and Aims

1. Introduction

The human mineral metabolism disorder, Idiopathic Infantile Hypercalcemia (IIH), is characterized by severe hypercalcemia, weight loss, dehydration, muscular hypotonia, lethargy, failure to thrive, vomiting and nephrocalcinosis [1]. The disease origins from the recessive mutations in *CYP24A1*the gene that codes for vitamin D-24-hydroxylase, the cytochrome P450 multi-catalytic enzyme that inactivates $1,25(OH)_2D_3$ by converting it into water-soluble calcitroic acid [2]. The mutations in the gene lead to disorder in vitamin-mineral homeostasis causing multi-systemic pathologies.

In this thesis, to better understand the disease, I will focus on the CYP24A1 mutations and its most common seen subgroup, R396W mutations.

A *Cyp24a1* knock out (KO) mouse model was previously generated by our research group, Dr. St-Arnaud's laboratory [3]. In this thesis, I will be providing my research on R396W-mutated mice based on the research schema previously done by Dr. Martineau et al. [4]

In the first chapter, I will provide a brief overview of bone physiology, bone and chondrocyte formation and maturation mechanisms, bone fracture repair, and its relationship to the vitamin D pathway. Also, I will explain vitamin D metabolism and IIH.

Second chapter will include the details of materials and methods that have been used in this research.

Finally, I will be presenting the results, discussing their relevance, and contributing the future directions.

1.1. The Skeleton and Bone Physiology

The adult human skeleton is composed of 206 bones in total which are classified in 3 parts. The appendicular skeleton holds 126 bones, the axial skeleton holds 74 and the last 6 ossicles are associated with auditory stimulus mechanotransduction. As one of the body's solid connective tissues, bone affords structural support, vital organ protection, and is responsible for the maintenance of mineral homeostasis and acid-base balance by holding the sufficient setting for hematopoiesis within the marrow spaces. In addition, it provides the attachment points to support ligaments and tendons to enable locomotion [5] and functions as a reservoir of the growth factors and cytokines [6]. Recent work has suggested that bone is also an endocrine tissue involved in the control of energy metabolism [7].

As a whole, bones are classified into four types: long bone, short bones, flat bones and irregular bones [5].

Bone structures can be broken down into two broad categories: the compact/cortical and the cancellous/trabecular. While both categories are composed of osteons, the composition of these osteons varies between categories. On cortical structures, osteons consist in osteocytes, and trabecular consist in packets, which are thin rods and plates that are aligned towards the areas that support the most stress. Also, while cortical structures are solid and found on the exterior layer of bones and represent 80% of the body's skeletal mass, trabecular structures are comparatively more flexible by virtue of their lower density. They represent 20% of the skeleton [5].

Note that human cortical bones are different from those of mice in several respects. In humans, the osteons are concentric layers of bone matrix involving osteocytes. These interact between each other over small canals designed around a vascular center [5, 8]. By contrast, in mice, cortical bones are composed of circumferential lamellae (thin layers of bone matrix) attached on the periosteal area. Unlike osteons, these are rarely remodelled [8].

1.2. Bone Development

Bone development is different for each of these types, even though they all contain the transformation of mesenchyme to bone tissue. For example, flat bones form by intramembranous bone formation, yet long bones evolve via endochondral ossification and intramembranous formation. Additionally, long bones have diaphysis and epiphyses, meaning a hollow shaft comprised of a cortical bone and composed by trabecular bone preserved by dense cortical bone found above the growth plates, respectively [5].

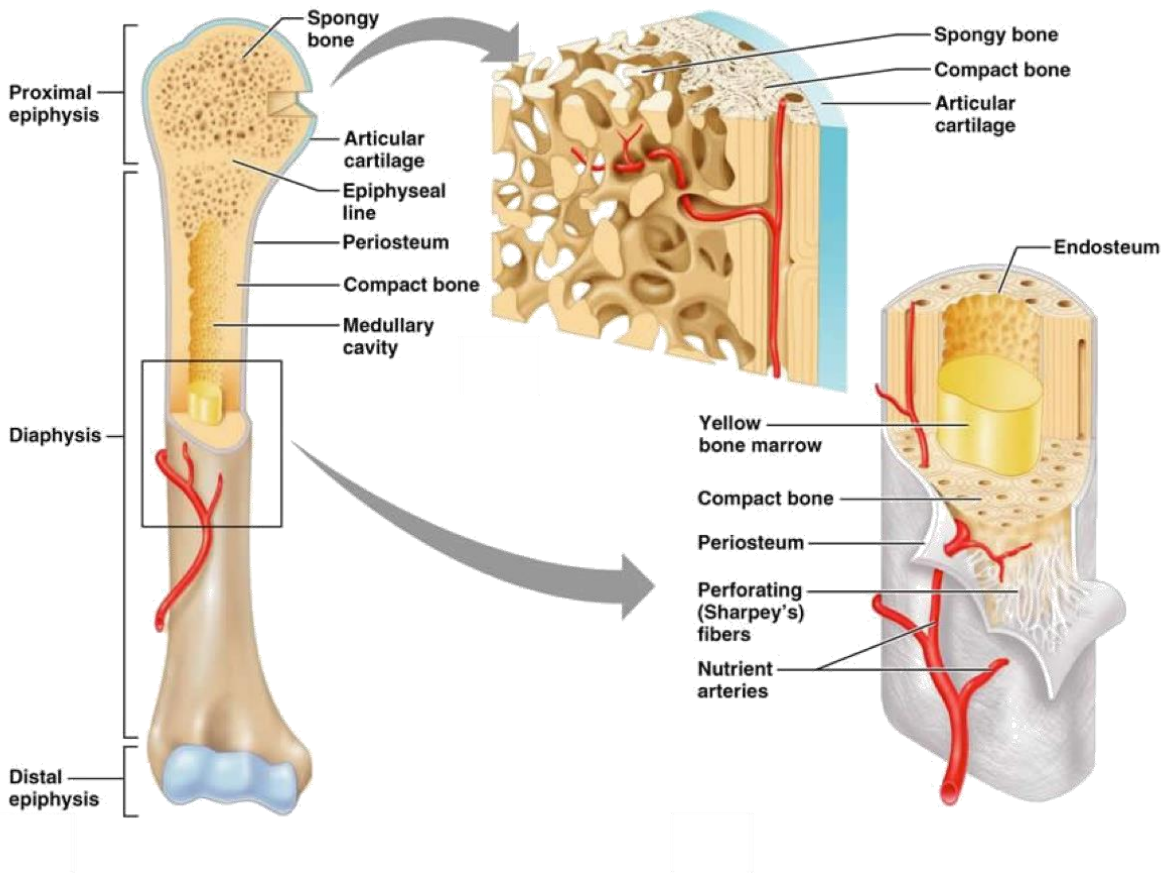

Figure 1. Macroscopic bone structure

The epiphysis, physis, metaphysis, and diaphysis are the primary areas of long bone. The periosteum, which is also a primary source of stem cells in fracture healing, supplies blood via nutritional arteries. At the physis, endochondral ossification occurs [9]. (2004 Pearson Education, Inc. Publishing as Benjamin Cummings)

1.3. Mineralisation

In bone, osteoblasts are mainly responsible for the secretion of several bone matrix proteins such as osteocalcin, osteonectin, type I collagen, biglycan, and decorin.

The mineralisation in the organic bone matrix starts when calcium restraint in the proteoglycan matrix and phosphate is discharged as a result of alkaline phosphatase activity, shaping hydroxyapatite crystals [10]. As osteoblasts secrete matrix, they could grow to be entrapped inside it and differentiate, turning into osteocytes. These extend long processes to communicate amongst themselves and thus reducing protein production. Acting as a mechanosensory organ, detecting pressure and loading, and communicating these data to other cells to guide bone adaptation are some of osteocytes' fundamental roles. Since osteocytes make up 90-95% of all bone cells, their spatial arrangement supports their function [10].

Osteoclasts, on the other hand, are multinucleated bone-resorbing cells of hematopoietic origin, instead of the mesenchymal origin of osteoblasts. They principally differentiate in the presence of macrophage colony-stimulating factor (M-CSF) and receptor activator of NFκB ligand (RANKL) [5, 10]. To initiate bone resorption, osteoclasts secrete hydrogen ions into the resorbing compartment to lower the pH of the tissue, optimising the activity of tartrate-resistant acid phosphatase, cathepsin K, matrix metalloproteinase 9 and gelatinase to absorb the organic matrix and mobilize the mineral [11].

1.3.1. Intramembranous Ossification

Skull, mandible, clavicles, and pelvis are the sites where intramembranous bone formation develops. It leads the surface of flat bones to grow and thicken [5]. The process begins by condensing and replicating mesenchymal stem cells (MSC), which are prevalent throughout an extracellular matrix (ECM) lacking collagen. They become osteoprogenitor cells as they become larger and rounder and have more Golgi apparatus and rough endoplasmic reticulum. As the process continues, the cells begin to drift outward, their shape resembles that of osteoblasts,

and the runt-related transcription factor 2 (RUNX2) is activated, causing them to commit [12]. Osteoblasts are able to secrete ECM containing type I collagen, forming osteoid, which mineralizes and forms rudimentary bone [13].

Bone spicules, also formed from differentiated osteoblasts, fuse together to construct the bone trabeculae. The woven bone generated by the junction of trabeculae will become filled as ossification progresses [12]. Woven bone is however weaker and immature as the collagen fibrils are secreted in a rather unorganized manner. Thus, the bone must be remodelled to produce a mechanically stronger, lamellar bone where collagen fibrils present alternating orientations [5, 12].

1.3.2. Endochondral Ossification

The presence of cartilaginous tissue distinguishes endochondral ossification from intramembranous ossification. The fetal skeleton is largely made up of cartilage, which will eventually turn into bone through endochondral ossification [14]. This type of ossification occurs in the vertebral column, pelvis, and limbs [12].

The development of a cartilage model that will eventually evolve into bone is the first stage of endochondral ossification. Mesenchymal cells condense to form cartilage, which then differentiate into chondrocytes and secrete ECM components. The activation of transcription factors paired box -1 (PAX1) and SCLERAXIS commits mesenchymal cells to the chondrogenic pathway, and they begin to express transcription factor Sex Determining Region related High Mobility Group box Gene 9 (SOX9) during the condensation stages [15, 16]. The creation of main and secondary ossification centers, which occur when a combination of cells invades the

network, will be aided by this cartilage lattice. The primary ossification center is found in the diaphysis, or shaft of the bone, whereas the secondary ossification center is found in the ends, or epiphysis of the bone, at the time of birth [17]. In mice, on the other hand, growth plate remainders stay all through life, although its thickness diminishes after 3 months of life where longitudinal development generally diminishes [8].

To allow longitudinal bone growth in a mechanically secure presence, some bones evolve in this aspect. Cartilage is found within the growth plate and the epiphysis of long bones, and it is organized on morphologically and practically definite areas. The resting chondrocyte zone is found the farthest from the solidification center, amplifying outwards towards the epiphysis. The proliferation comes next, where chondrocytes go through mitosis, smooth, and adjust into stacks. Usually taken after by the zone of hypertrophy, where chondrocytes end up profoundly extended in size and secrete ECM characterized by collagen type II and X, fibronectin and alkaline phosphatase [17]. The ECM gets to be mineralized and hypertrophic chondrocytes in this zone perish as they cannot receive supplements or eliminate squander effectively within the zone of calcification. The cavities cleared out by these apoptotic cells are filled with attacking blood vessels, osteoclasts, osteoprogenitors and bone marrow cells. Osteoclasts resorb the cartilage matrix and osteoprogenitors differentiate into osteoblasts, which secrete ECM that will end up mineralized and renovated within the ossification zone [17].

Finally, growth happens in the presence of cartilage in the bone tissue. That can be in two ways, interstitial, and appositional growth. Interstitial growth, also called longitudinal, exists when chondrocytes segregate and remain excreting the matrix. Oppositional growth, on the other

hand, is the increase in the diameter or thickness by addition of ECM by chondroblasts and osteoblasts [12].

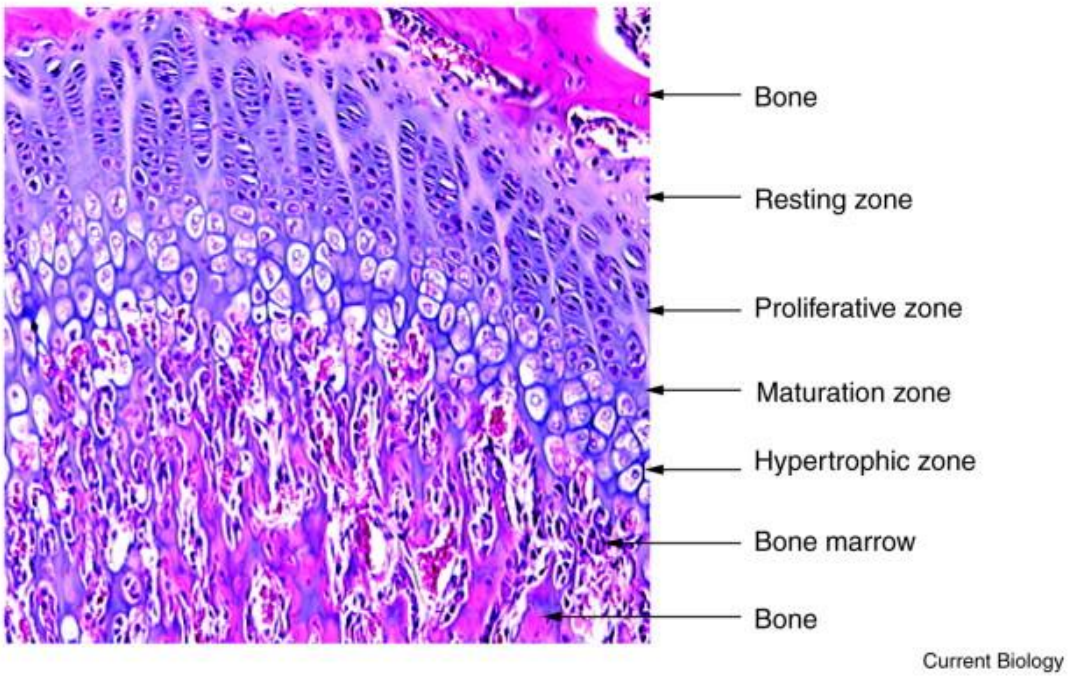

Figure 2 Endochondral ossification and cartilage differentiation

At the physis, chondrocytes undergo proliferation, hypertrophy, and death during endochondral ossification. The mineralized matrix that remains is infiltrated by blood vessels. Osteogenesis is aided by growth factors such as growth hormone, thyroid hormone, and FGF23. To govern and regulate chondrocyte proliferation and hypertrophy, Indian hedgehog and PTHrP form a feedback loop. This procedure is necessary for fracture healing as detailed in this thesis. Figure adapted from White et al. (2001) [18], with permission.

1.4. Chondrocyte Differentiation

Articular cartilage is a solid connective tissue that is devoid of nerves, blood vessels, or lymphatic vessels. In joint movement, it acts as a load bearing, buffering, and protective structure [19, 20]. Chondrocytes are the only cell type in the articular cartilage tissue and release growth factors and enzymes that govern ECM formation. They continue to embed themselves in the ECM, forming cartilage [21]. Collagen type II and aggrecan (ACAN), two main ECM components, are classic chondrocytic phenotype markers. The ECM network oversees absorbing articular cartilage mechanical stress, increasing chondrocytes adhesion, and controlling intracellular signal transduction [20].

Chondrocytes develop from bone marrow mesenchymal stem cells (BMSCs) in the bone marrow. To begin with, aggregated BMSCs can differentiate into chondroprogenitor cells the differentiate into chondrocytes, which then undergo a series of differentiation events to become hypertrophic chondrocytes. After apoptosis and endochondral ossification, chondrocytes are gradually replaced by osteoblasts as the cartilage matrix becomes partially calcified. Although chondrocyte hypertrophy and apoptosis are natural processes of endochondral ossification, when cartilage is damaged, they will hasten the progression of osteoarthritis (OA) [22]. Furthermore, chondrocytes cultured in vitro have a highly susceptible growth and differentiation regulation mechanism, which can readily lead to cell ageing and differentiation. Differentiation of chondrocytes is followed by changes in fibrous phenotype, decreased collagen II expression, and increased collagen I, matrix metalloproteinase 13 (MMP-13), and nitric oxide synthase (NOS) production [20, 23, 24].

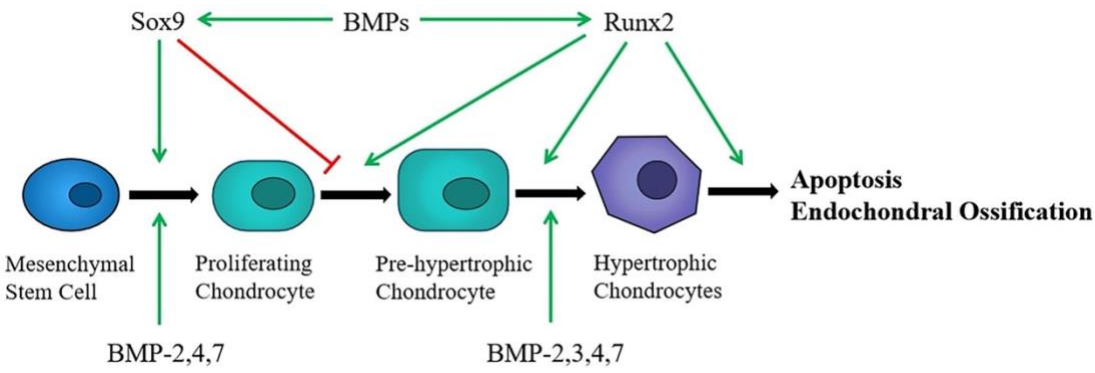

Figure 3 Generation of hypertrophic chondrocyte

MSCs evolve to chondrocytes, which go through a series of transformations. Sox9 enhances MSC proliferation and differentiation into chondrocytes, whereas Runx2 stimulates chondrocytes ends in hypertrophy. BMPs regulate the expression of Sox9 and Runx2 and alter various stages of chondrocyte development.

The ability to regenerate and repair cartilage is severely limited. It is nearly impossible for cartilage to self-heal once it has been damaged, and it may even deteriorate. Cartilage repair is not efficient but involves chondrocyte proliferation and ECM synthesis [25]. The proliferation, metabolism, and differentiation of chondrocytes is a sophisticated process. Several cytokines and cellular signals cooperate to maintain cartilage homeostasis and regulate chondrocyte function [20, 26].

1.5. Bone as an Endocrine Organ

Bone has traditionally been thought of as a structural organ that develops as a result of the activity of specialized cells such as chondrocytes and osteoblasts. Osteoblasts produce bone matrix and eventually get encased in it to become osteocytes, cells that operate as gravity force sensors and mediators within the remodelling unit [27, 28]. In addition to being a structure for

mobility, calcium homeostasis and haematological function are all dependent on bone. The role of the skeleton as an endocrine organ has recently been highlighted by breakthroughs in bone biology [29].

There are numerous bone cell hormones identified previously. Such as sclerostin, an osteocyte-released bone-specific protein that might have a function as a paracrine inhibitor of osteoblast differentiation [30]. Furthermore, it was previously recognised that osteocytes produce and secrete fibroblast growth factor-23 (FGF-23) into the circulation, a key regulator of vitamin D-1-alpha-hydroxylase, PTH and serum phosphate homeostasis [31] (fig. 4).

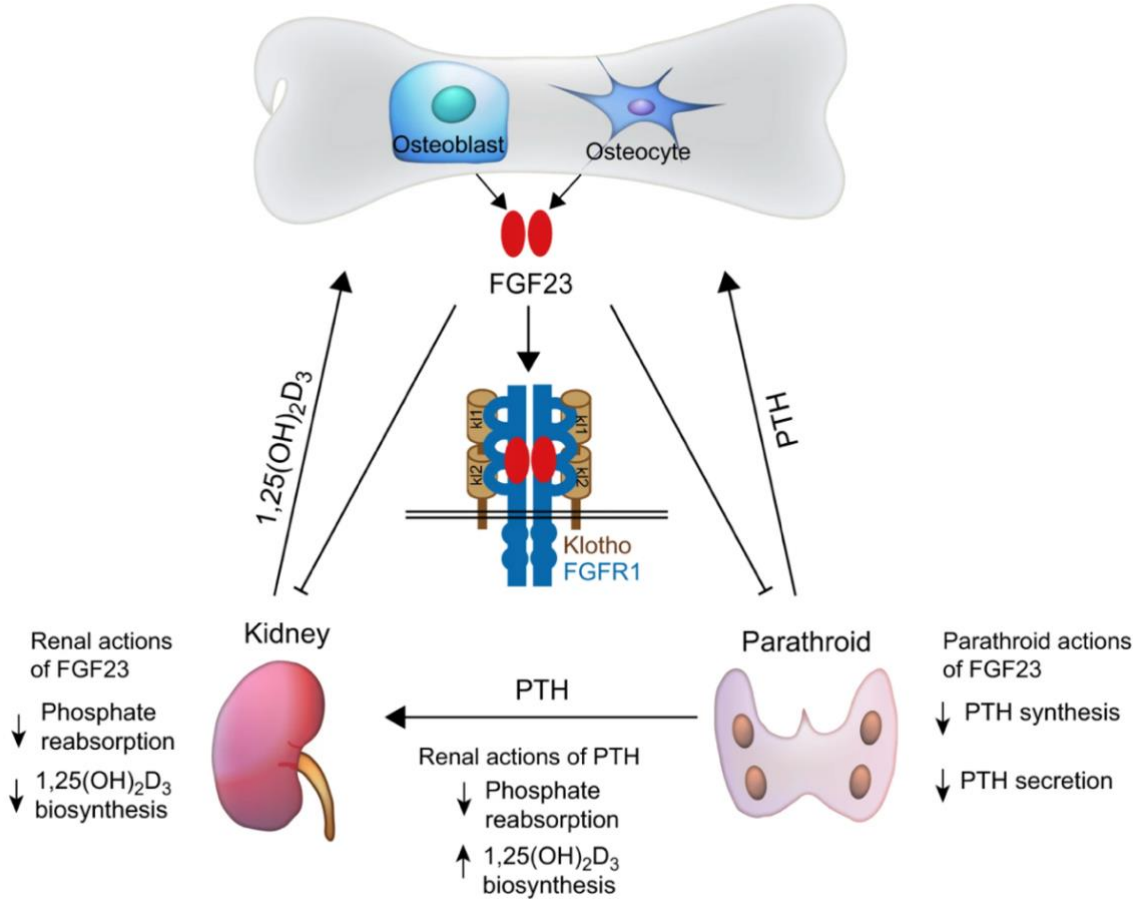

Figure 4 FGF23 is a bone derived protein that affects phosphate metabolism

Through its binding to a complex of FGFR1 and the co-receptor Klotho in the kidney, FGF23, inhibits phosphate resorption and reduces the synthesis of 1,25(OH)2D3. in the parathyroid, FGF23 decreases PTH production and secretion in a Klotho-dependent manner. 1,25(OH)2D3 and PTH both influence FGF23 synthesis and secretion in osteoblasts and osteocytes. PTH, can inhibit phosphate resorption and 1,25(OH)2D3 synthesis in the kidney [32]. (Copyright 2018, Yujihao Han et al.)

In addition to its role in mineral metabolism, bone could function as a mediator to metabolic homeostasis by its specific protein, osteocalcin (OCN). It is a bone-derived hormone that affects the biological processes of various organs, including liver, bone, adipose, brain testes, muscle and, pancreas [32-34] (Fig. 5). Furthermore, new research shows that osteoblast-derived lipocalin-2 (LCN2) modulates glucose tolerance, insulin sensitivity, and insulin secretion to maintain glucose homeostasis by binding protein to the melanocortin 4 receptor (MC4R) in the hypothalamus and inhibiting food intake [32, 35] (Fig. 6).

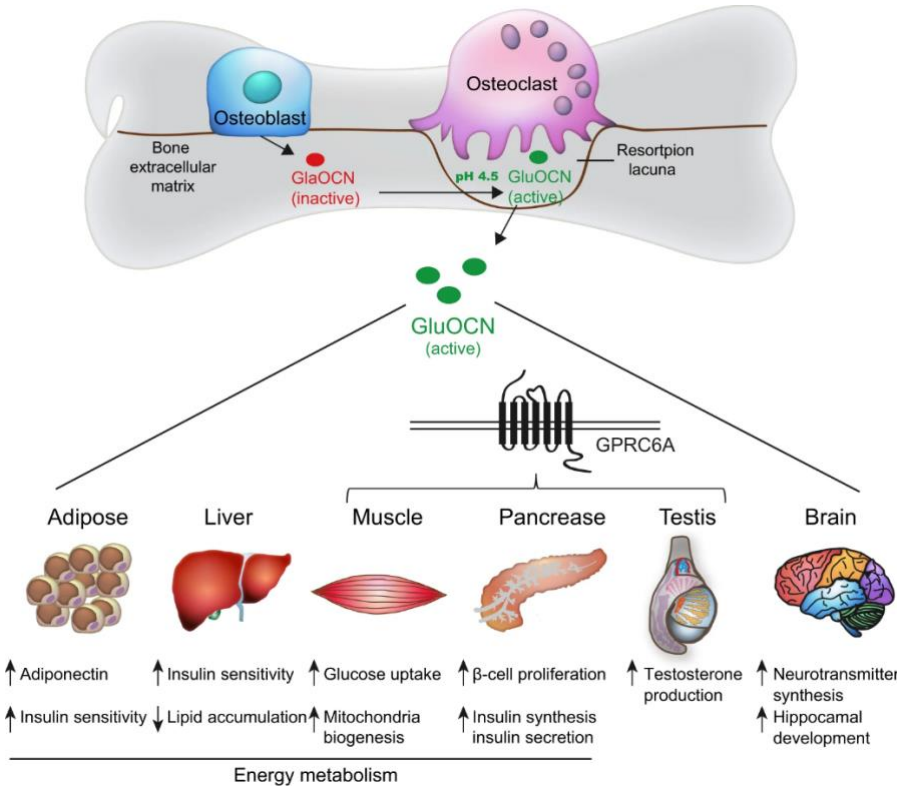

Figure 5 OCN is a multifunctional hormone generated from the bones

OCN is C-carboxylated (GlaOCN) and secreted into the extracellular matrix (ECM) of bone by osteoblasts. GlaOCN is decarboxylated into undercarboxylated active osteocalcin (GluOCN), which enters the blood to act as a hormone, due to the acidic pH (4.5) in the resorption lacunae generated by osteoclasts. Enhancement of glucose uptake in muscle, insulin generation in the pancreas, insulin sensitivity in the liver and adipose tissue, elevation of adiponectin expression in adipose tissue, and promotion of b-cell proliferation in the pancreas are all regulated by GluOCN. Furthermore, OCN increases cognitive function of the brain by increasing neurotransmitter synthesis and facilitating hippocampal growth by stimulating testosterone synthesis in Leydig cells, which improvise male fertility. OCN acts in the testis, pancreas, and muscle via binding to the GPRC6A receptor, although OCN receptors in the brain, adipose tissue, and liver are still unknown [32]. Copyright 2018, Yujihao Han et al.

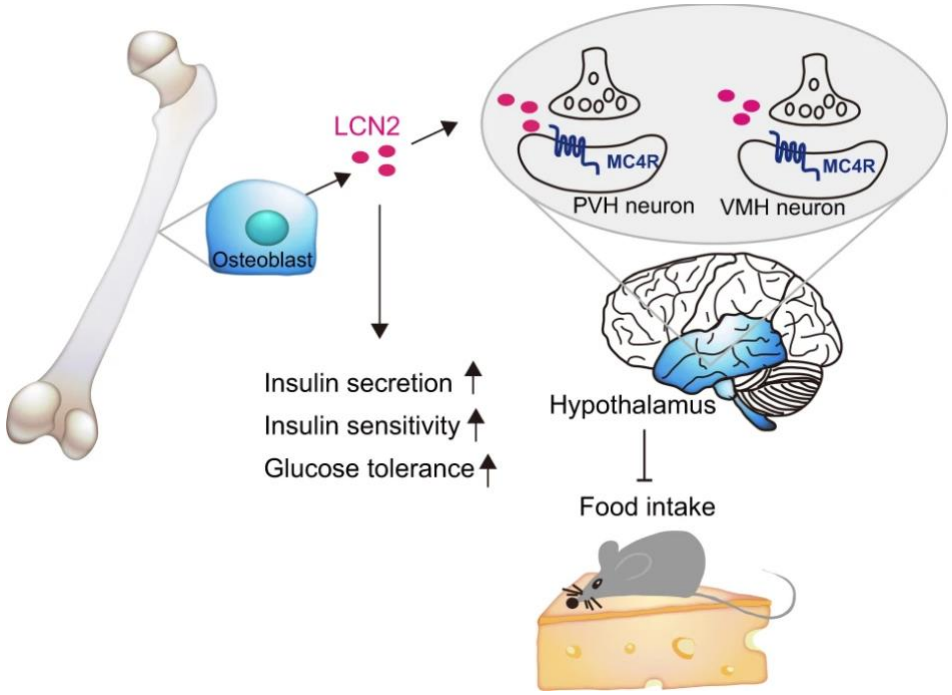

Figure 6 Food intake suppressed by osteoblast derived LCN2

LCN2 produced by osteoblasts and crosses the blood-brain barrier to reach the hypothalamus, where it binds to the MC4R receptor in the paraventricular nucleus (PVN]) and ventromedial hypothalamus (VMH) and triggers MC4R-dependent anorexigenic signalling. LCN2 is also involved in the regulation of glucose tolerance, insulin sensitivity, and insulin secretion [32]. Copyright 2018, Yujihao Han et al.

Bone is also having a role as a target organ of several endocrine glands and tissues such as glucagon-like-peptides-1 (GLP1), PTH, adipokines and immune cell-produced cytokines.

1.6. Fracture Repair Stages

Bone fracture healing is a complex process that requires the tightly ordered cooperation of cells, growth factors, and extracellular matrices [14]. Bone fracture healing is categorized as

primary or secondary, due to underlying healing mechanisms relying on rigidity of the fracture construct. Primary healing occurs when bone fragment are in direct contact with one another and highly stable with minimal strain [14]. Haversian remodelling aids fracture healing by relying on osteoclasts and osteoblasts to directly rebuild the bone fragments. Secondary healing is more common and is characterized by four steps: 1) the initial inflammatory phase, 2) soft callus formation, 3) hard callus formation, and 4) remodeling [36].

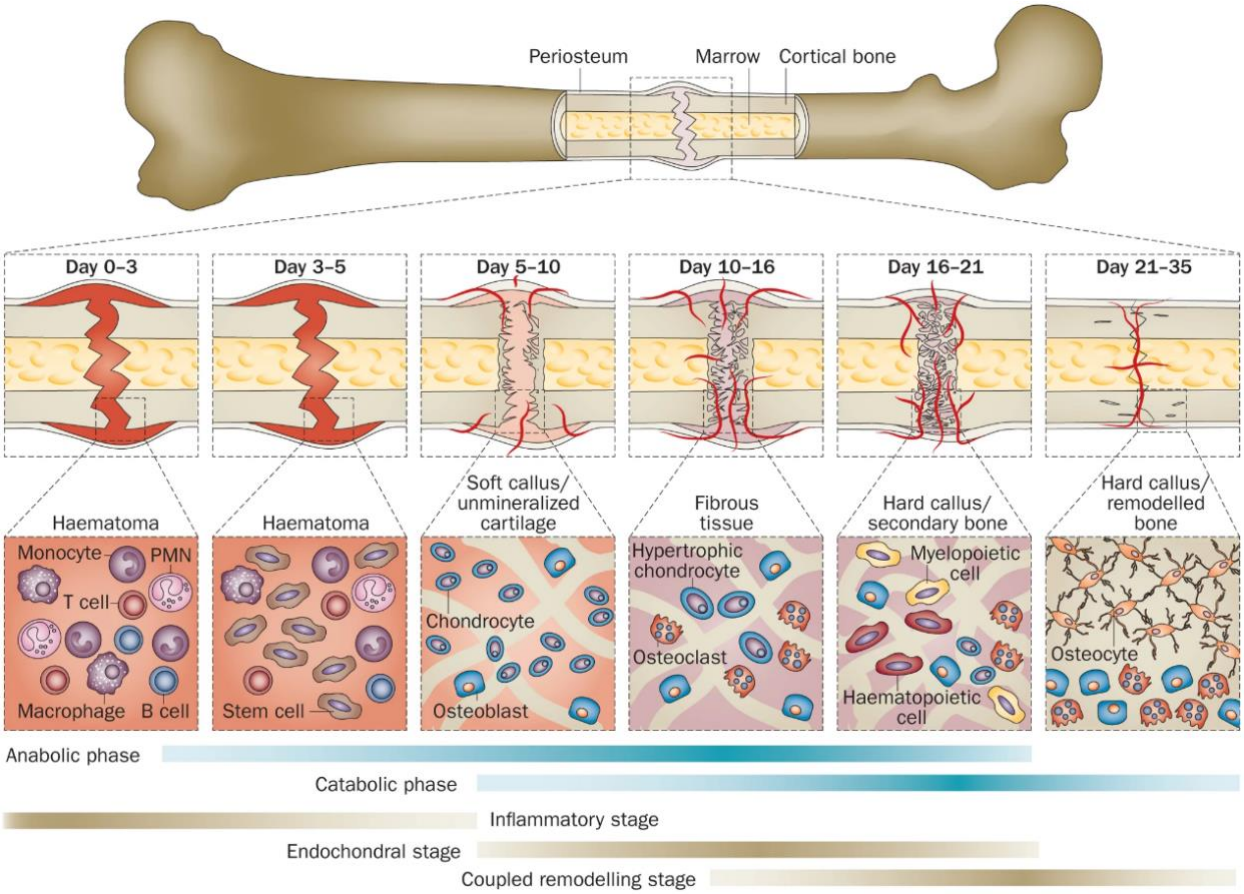

Figure 7 Phases of normal fracture healing

Secondary fracture healing is depicted as a step-by-step process that restores the bone's natural strength and shape without leaving a scar. The presence of hematoma from broken blood arteries

generates a clot during the inflammatory phase, which attracts immune cells and, mesenchymal progenitor cells via inflammatory signalling. The bone gap is bridged by a soft callus, which is mostly formed of cartilage. The process of endochondral ossification leads to the production of new bone. Remodelling by osteoclasts and osteoblasts restores the normal shape of the bone. Figure adapted from Einhorn et al.(2014) [37], with permission.

The early inflammatory phase of secondary fracture healing is crucial to the entire healing process [38]. When the inflammatory cascade is triggered, endothelial, neuronal, and mesenchymal stem/progenitor/precursor cells are brought into the site of injury, leading to formation of a vascularized and innervated fibrous granulation tissue [36]. As macrophages, neutrophils, lymphocytes, and platelets arrive at the injury site and release cytokines, inflammation begins, peaking at 24 hours. Initially haematoma occurs when blood vessels in the bone and surroundings soft tissue are disrupted, triggering an inflammatory response. Transforming growth factor beta (TGF- β), Insulin-like growth factor (IGF) and FGFs released by macrophages recruit mesenchymal cells to the injury site [38, 39]. Immune cells drawn to the injury site generate growth factors and cytokines such as TNF- α, interleukin -1 beta (IL-1β), IL-6, and monocyte chemoattractant protein-1 (MCP-1), which attract mesenchymal stem cells from periosteum, bone marrow, and the systemic circulation [40, 41]. The proliferation in MSCs starts within 3 days post-fracture and differentiates into chondrocytes following nearly 21 days. The hematoma and inflammatory reaction support chondrogenic and osteogenic differentiation, which ultimately leads to soft callus formation.

The soft callus is made up of cartilage and granulation tissue, and it serves as a biologic scaffold for the formation of new bone. Chondrogenic maturation remains to enable bone

formation. The steps are proliferation, hypertrophy, apoptosis, followed by vascular invasion. On the scaffold of destroyed chondrocytes, osteoblasts form primary bone that turns into a hard callus. And finally, the remodelling phase, the last phase of fracture healing process, takes longer duration according to the other phases. This phase also includes the remodelling of the woven bone and formation of the lamellar bone. The remodelling of the medullary canal and endosteal callus to allow for reconstitution of the bone marrow also appears in this phase. The optimum bone renewal includes its original strength, histology, and physiology. The duration and the healing status depend on the age, the injury site, comorbidity, sex, and other health condition [36].

Beside the factors mentioned earlier, signaling pathways have a particular role during the fracture repair. They include MAPK (mitogen-activated protein kinase), WNT/β-catenin, Notch, BMP (bone morphogenic protein) and PDGF (platelet derived growth factor) [36]. The MAPK pathway has a crosstalk role in other pathways and transduces the epidermal growth factor (EGF), FGF and IGF signals in bone healing [36]. It can be also triggered by some inflammatory markers such as TNFα and NF-κB [39, 42]. In osteoblasts, this pathway has been demonstrated to have opposing effects on osteoblast differentiation and osteoblast marker gene expression [43]. Canonical WNT signaling is activated during bone healing and enhances osteoblastogenesis. This stimulates MSC differentiation into osteoblasts during fracture repair [44] . The other factor that is necessary for MSC differentiation into osteoblasts is Notch signaling. The inhibition of this pathway could cause non-union via reducing the MSCs derivation from bone-marrow [45, 46]. BMP signaling is important to activate endochondral bone formation, thus, osteogenesis advancement [47]. Through differentiation of MSCs of bone marrow origin into osteoblasts and through the chemotaxis attraction of macrophages, PDGF

signalling has a role in bone repair [48]. While the IGF pathway leads the osteoblast differentiation, matrix deposition and expression of type I collagen, the FGF pathway has a role in angiogenesis, wound healing and intramembranous and endochondral signaling in osteoprogenitor cells [49-51].

1.7. Vitamin D

The discovery of vitamin D is linked to the search for a remedy for a disease called rickets. The search for the cure to this endemic disease during the beginning of the 19th century, firstly led the use of the cod fish oil and finally ended by the discovery of Vitamin D in 1820s. The use of vitamin D as a nutritional supplement succeeded to lower the incidence of the two seriously damaging bone diseases, rickets and osteomalacia.

Vitamin D is an essential molecule in bone metabolism and has numerous roles in many cellular and immunological processes. It can be either synthesized in the body or consumed through the diet.

1.7.1. Vitamin D forms and sources

In humans, the synthesis of vitamin D in the skin via exposure to the sun's ultraviolet B (UVB) light is the most generous source of their vitamin D [52]. In addition to the endogenous production in the skin, there are also plant (vitamin D_2 or ergocalciferol), or animal vitamin D (vitamin D_3 or cholecalciferol) forms. The main differences between these two forms rely on the presence of a double bond between C-22/C-23 and a methyl group bound to C-24 (fig. 8). Even though some of the hydroxylating enzymes could use vitamin D_2 as a substrate, both metabolites don't follow the same metabolic pathways [2].

Some of the best natural sources of vitamin D_3 are fatty fish, such as fresh wild salmon (can produce nearly 600-1000IU of vitamin D_3 per 100 gram serving) and fish oils, such as cod liver oil (400-1000 IU of vitamin D_3 per 1 tablespoon) [52]. Among plants, sun-dried mushrooms are a rich source of vitamin D_2 (1600 IU of vitamin D_2 per 100 gr of sun dried shiitake mushrooms) [52].

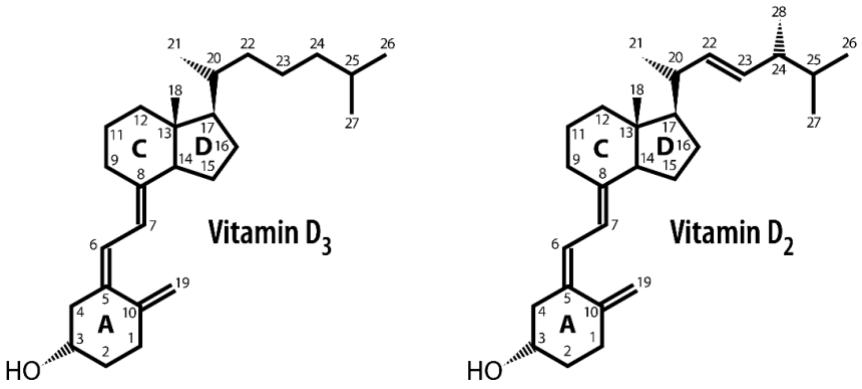

Figure 8 Vitamin D3 (cholecalciferol) and D2 (ergocalciferol)

Different than cholecalciferol, ergocalciferol (vitamin D2) has a double bond at C-22 and a methyl group at C-24.

Due to limited food sources of vitamin D and their lack in diets, several countries routinely fortify certain food sources with vitamin D such as fluid milk products, margarines, plant milk products etc. [53].

1.7.2. Vitamin D metabolism

Vitamin D can be synthesized upon exposure of ultraviolet B (UVB) photons in both animals and plants, through UVB photoisomerization of provitamins. In plants and fungi,

synthesis happens in basically a similar way upon exposure to UVB, although provitamin D_2 or ergosterol (and not 7DHC) is the forerunner of vitamin D combination in plants and organisms, and the subsequent nutrient D_2 is ergocalciferol [52].

In mammals, vitamin D is synthesized from provitamin D_3 (7-dehydrocholesterol (7DHC)) which is found in large quantities in the skin of many vertebrate animals, including humans [52]. Exposure to sunlight triggers the high-energy UVB photons to penetrate the epidermal and dermal cells of the skin and are absorbed by 7DHC and this reaction results in creation of previtamin D_3 (from the precursor 7DHC) [54]. From this thermodynamically unstable form (previtamin D_3) a rearrangement occurs with cleavage at the B ring to produce a more stable form, vitamin D_3 (cholecalciferol). Vitamin D_3 infuses into the dermal capillary bed by the vitamin D-binding protein (VDBP) and makes its way to the circulation [55].

To form the physiologically active hormone, $1,25(OH)_2D_3$, vitamin D must undergo two hydroxylation steps after entering the circulation. An endocrine mechanism or a more recently suggested autocrine pathway can cause these effects [56].

In the well-known endocrine pathway, circulating vitamin D_3, cholecalciferol, from all sources is transported to the liver. It is hydroxylated in liver hepatocytes by the high affinity CYP2R1 enzyme (vitamin D_3 25-hydroxylase) or by the lower affinity CYP27A1 enzyme at the 25^{th} carbon to form 25-hydroxyvitamin D_3 (called calcifediol or $25(OH)D_3$). In the circulation, calcifediol is bound by D-binding protein (DBP), an α-globulin that increases its solubility. The production of $25(OH)D_3$ in the liver is not highly regulated. Cholecalciferol found in the circulation can readily be converted into $25(OH)D_3$ in a concentration-dependent manner, which can be used to measure vitamin D status in clinic. DBP-$25(OH)D_3$ is transported throughout the

body, where it is hydroxylated at the 1-α position by the CYP27B1 enzyme (25-hydroxyvitamin D_3 1-alpha-hydroxylase) in the kidney proximal tubules to create calcitriol or $1,25(OH)_2D_3$. The action of this enzyme is strictly regulated by the body's calcium and phosphorus requirements [2].

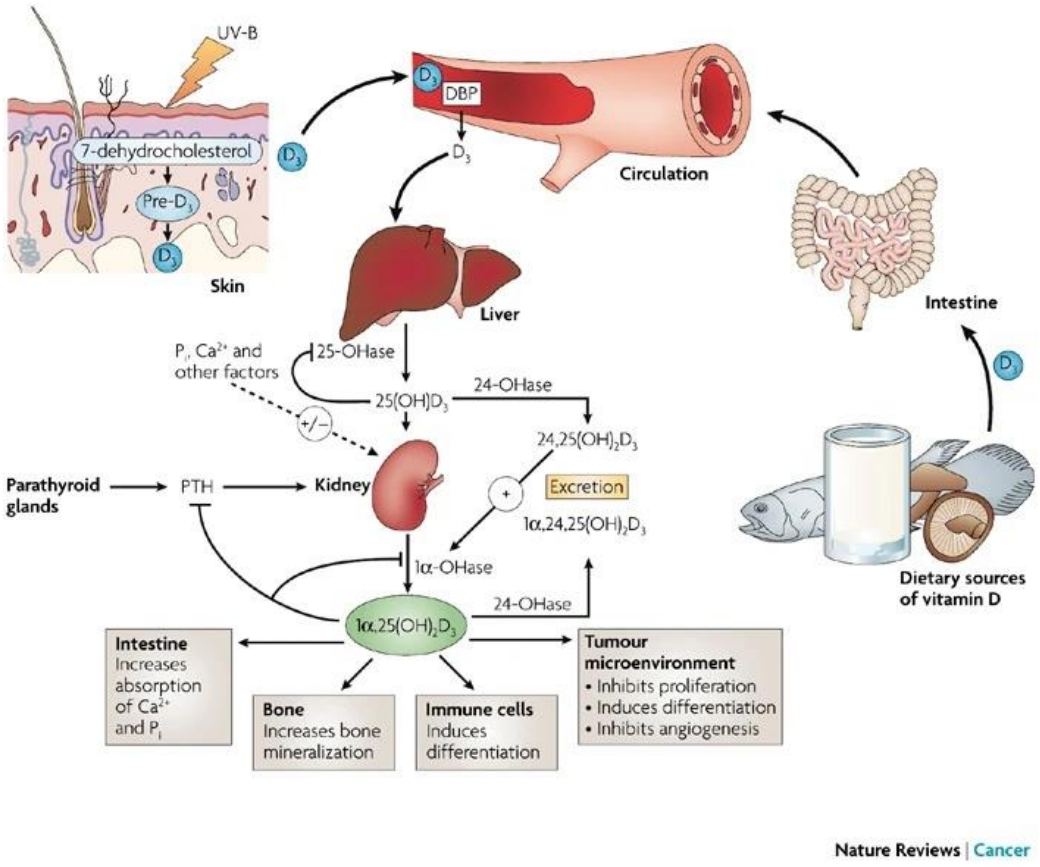

Figure 9 Vitamin D pathway with the key enzymes and metabolites produced

Figure adapted from Deeb et al. (1969) [41], with permission.

In the presence of biologically sufficient amounts of $1,25(OH)_2D_3$ in the circulation, previtamin D_3 and vitamin D_3 are transformed by solar UVA or UVB to a variety of inert by-products, therefore excessive sunlight exposure cannot lead to overproduction of the biologically

active $1,25(OH)_2D_3$, which is toxic at high concentrations [57]. The normal concentration is within the 20 to 65 ng/mL range [2].

1.7.3. Vitamin D and VDR signaling

The most active form of vitamin D is $1,25(OH)_2D_3$ and it works by diffusing through the cell membrane an attaching to the vitamin D receptor (VDR), a ligand-activated transcription factor that belongs to the nuclear receptor family. VDR and the retinoid-X receptor (RXR) form a heterodimer and bind the vitamin D-responsive regions of target genes. The parathyroid gland, pancreas, macrophages, skin keratinocytes, mammary glands, reproductive organs, tubular epithelial cells of the kidney, osteoblasts, and osteoclast precursors are all reported to express VDR [2].

Mutations on the vitamin D metabolic pathway enzymes cause different hereditary pathologies. 7-Dehydroholesterol reductase (DHCR7) enzyme polymorphisms, for example, are linked with low 25OHD levels, and inactivating mutations manifest with high vitamin D [58]. CYP2R1, which is the major vitamin D 25-hydroxylase, inactivating mutations develop a rickets form called vitamin D-dependent rickets, type 1B (VDDR1B) [59]. VDDR1B manifests in the affected individuals with low 25OHD but normal $1,25(OH)_2D_3$ levels. It is also associated with hypocalcaemia, hypophosphatemia, and infantile onset. The disease responds to 25OHD (calcidiol) treatment and does not require treatment as adults. Mutations in the CYP27B1 enzyme are characterized by another form of rickets, pseudo vitamin D deficiency rickets or vitamin D-hydroxylation deficient rickets (VDDR1A) [60]. The affected individuals have similar clinical symptoms as VDRR1B patients but have lower $1,25(OH)_2D_3$ and normal 25OHD levels. VDRR1A responds to calcitriol. CYP24A1 enzyme mutations result in a form of idiopathic

infantile hypercalcemia (IIH) [1, 61]. It is characterized with hypercalcemia in children and kidney stone history and elevated $1,25(OH)_2D_3$ levels in adulthood. The discoveries of the mutations and association with the adult life changed the approach to the IIH disease. It is no longer idiopathic, and also not only seen in childhood [61]. The disease and mutations on CYP24A1 will be mentioned in detail later in this thesis.

1.7.4. Role in Calcium Homeostasis

The production of $1,25(OH)_2D_3$ by CYP27B1 is regulated by the parathyroid hormone (PTH) in response to circulating calcium and phosphate levels. Low levels of those ions trigger the PTH release which stimulates $1,25(OH)_2D_3$ production. $1,25(OH)_2D_3$ in turn stimulates calcium and phosphorus absorption in the small intestine. It promotes calcium reabsorption in the kidney's distal convoluted tubules. PTH stimulates RANKL expression by osteoblasts, which accelerates osteoclastogenesis and bone resorption, mobilising calcium from bone [62]. Although $25(OH)D_3$ is not the natural ligand of the VDR, it can compete with normal amounts of circulating $1,25(OH)_2D_3$ and cause effects generally attributed to it when it is circulating at high quantities (1000 ng/mL or above), such as in vitamin D toxicosis [55].

PTH expression is inhibited by $1,25(OH)_2D_3$ in the parathyroid gland to prevent CYP27B1 stimulation [55]. In a negative feedback loop, $1,25(OH)_2D_3$ also promotes fibroblast growth factor 23 (FGF23) secretion, which stimulates phosphate excretion from the body while decreasing CYP27B1 activity. Osteocalcin and osteopontin, which are involved in bone remodelling, are transcriptionally activated in osteoblasts, while involucrin and carbonic anhydrase are active in keratinocytes and macrophages, respectively [62].

CYP24A1, the gene that encodes 1,25-dihydroxyvitamin-D_3 24-hydroxylase, is responsible for hydroxylating $1,25(OH)_2D_3$ and its precursor $25(OH)D_3$ at the 24^{th} carbon, resulting in 1,24,25-trihydroxyvitamin D_3 ($1,24,25(OH)_3D_3$) and 24,25-dihydroxyvitamin D_3 (also known as secalciferol or $24,25(OH)_2D_3$). Until recently, $24,25(OH)_2D_3$ was a metabolite largely believed to be inactive. The carbons located in the side chain, specifically C-23, C-24, C-26, are more prone to being hydroxylated. These metabolites can be metabolized further to produce calcitroic acid, which is water-soluble and eliminated from the body [55].

1.8. CYP24A1 and 24,25(OH)2D3

The stereospecific hydroxylation of the 24^{th} carbon of $1,25(OH)_2D_3$ and $25(OH)D_3$ is carried out by CYP24A1, a heme-containing cytochrome P450 enzyme located in the inner membrane of mitochondria of humans and other species. It is thought to be a catabolic enzyme since $1,25(OH)_2D_3$ induces its expression to regulate its breakdown and prevent hypervitaminosis D [55]. In vitro studies of the activation of *Cyp24a1* by $1,25(OH)_2D_3$ revealed that the promoter of this gene has two VDREs 100bp apart in the non-coding section, a tandem structure unique to this promoter [63]. Recent research has revealed a more complicated control of *Cyp24a1* expression in vivo [64, 65].

Because $25(OH)D_3$ is more common in the body and has a lower Michaelis constant (*K*m) than $1,25(OH)_2D_3$, the primary metabolite generated is $24,25(OH)_2D_3$. Furthermore, $1,24,25(OH)_3D_3$ is unstable in the circulation and has a greater affinity to CYP24A1, causing it to bind to the enzyme and be rapidly destroyed. In the plasma, $24,25(OH)_2D_3$ circulates at a concentration of 2-5ng/mL, which is 10-fold lower than circulating $25(OH)D_3$ [55].

CYP24A1 initiates a reaction process in which its substrates are hydroxylated and then oxidised at carbon 24, followed by hydroxylation of the 23rd carbon and cleavage of the side chain to produce the ultimate degradation product, calcitroic acid. Calcitroic acid is water soluble, which means it can be excreted (figure 10). CYP24A1 is classified as a multi-catalytic enzyme since it can execute multiple steps in the degradation of 24,25(OH)2D3. Although human CYP24A1 is primarily a C24-oxidation enzyme, it can also express C23-hydroxylation activity, which results in lactone and carboxylic acid as end products. Point residue variations in the enzyme's substrate binding and catalytic core determine this differential in activity [66].

Cyp24a1 expression is induced by $1,25(OH)_2D_3$ in all target tissues. This activates the 24-oxydation pathway, which results in catabolic inactivation of $1,25(OH)_2D_3$, allowing vitamin D homeostasis to be maintained. PTH and $1,25(OH)D_3$ concentration are the major regulators of CYP24A1 activity in the kidney [2, 67]. PTH treatments prevents the $1,25(OH)_2D_3$ -mediated rises in renal *Cyp24a1* mRNA expression, whereas $1,25(OH)_2D_3$ administration increases renal *Cyp24a1* mRNA expression [68, 69]. Because intestine cells lack a PTH receptor, *Cyp24a1* is predominantly controlled by $1,25(OH)_2D_3$ in the gut. The injection of $1,25(OH)_2D_3$ stimulates intestine *Cyp24a1* expression, causing it to catabolize, and this response is more severe than one seen in the kidney [70]. *Cyp24a1* expression is higher in mature osteoblasts than in younger ones in response to $1,25(OH)_2D_3$, but expression declines in differentiated mature cells, limiting $1,25(OH)_2D_3$ breakdown as osteoblasts mature. In macrophages, interferon-gamma (IFNγ) stimulates the production of $1,25(OH)_2D_3$ by raising *Cyp27b1* expression and suppressing *Cyp24a1*, affecting the ability of $1,25(OH)_2D_3$ to regulate itself.

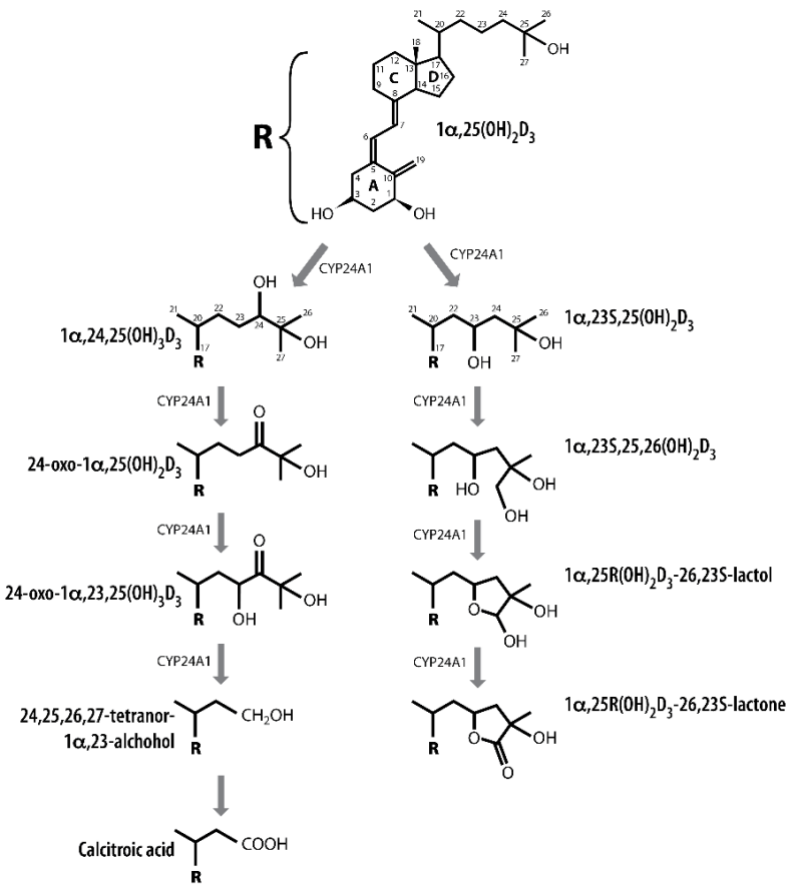

Figure 10 The catabolism of 1,25(OH)2D3 by CYP24A1

First branch shows the forming of calcitroic acid by oxidization at C-24 and hydroxylation at C-23. Second branch shows the lactone and carboxylic acid pathway hydroxylation C-23. [1]

The *CYP24A1* gene is present on chromosome 20 in humans and the mutation in the gene causes a disease called Idiopathic Infantile Hypercalcemia (IIH) which occurs mostly in infants. Dehydration, failure to thrive, weight loss, fever, and vomiting are the common symptoms. Also, it manifests with high vitamin D levels, hypercalcemia, low PTH, nephrocalcinosis, and hypercalciuria [1]. We mention more about this disease in the following sections.

1.9. Idiopathic Infantile Hypercalcemia (IIH)

Idiopathic infantile hypercalcemia (IIH) was first reported by Lightwood in the 1950's in the United Kingdom. An elevation of the number of IIH cases was observed following introduction of an increased prophylactic dose of vitamin D in infant formula and milk products [71, 72]. The infants were found to have high levels of serum and urinary excretion of calcium, and physiologic levels of serum phosphate and magnesium and occasionally low serum alkaline phosphatase (ALP). Halving the vitamin D dose lowered the observed incidence. Lightwood afterwards hypothesized fluctuation in infants' sensitivity to vitamin D due to unaffected cases during the treatment.

The general manifestations of this rare disease are high serum calcium and high urinary calcium loses, failure to thrive, vomiting, constipation, polyuria with dehydration and Ca deposits in the kidney, with a susceptibility to renal complications such as nephrolithiasis (NL) or nephrocalcinosis (NC). Affected infants may also manifest muscular hypotonia and lethargy, which leads to growth impairment, delays in mental and mobility development [73]. Affected adults could also manifest some extra-renal pathologies, such as Ca deposits in the joints and in the cornea, a low bone mineral density with osteoporosis, mainly based on enhanced osteoclastic activity [74, 75]. The genetic cause of IIH remained unknown until Schlingmann and coworkers identified it in 2011. They found inactivating mutations in *CYP24A1* that appeared to drive the disease evolution [1]. They furthermore characterized a disease subgroup that presented idiopathic renal Pi depletion in addition to the other typical IIH traits, without carrying *CYP24A1* mutations. In these patients, the pathology was caused by *SLC34A1* genetic variants. In this new study, the clinical and biochemical pathologies remained following the cessation of vitamin D

prophylaxis while a sudden response to Pi registration emerged, contradictorily to the *CYP24A1* mutated patients [76]. These findings, which confirm the significance of *SLC34A1* as a substitute genetic cause of IIH, highlight the disease's molecular heterogeneity and provide another avenue for increasing the number of individuals for whom a specific molecular diagnosis can be made.

1.10. *Cyp24a1-null* Mice

Using embryonic stem cell technology, the St-Arnaud lab created a knockout (KO) mouse model for CYP24A1 by replacing the heme-binding domain of *Cyp24a1* on exons 9 and 10 with a PGK-neo (phosphoglycerate kinase promoter driving the neomycin phosphotransferase II gene) selection cassette. The heterozygous offspring are phenotypically normal, and the mutation is passed down with the usual Mendelian ratio. However, at roughly 3 weeks of age, half of the mutant progeny dies. The function of macrophages was studied to rule out an inadequate response to infection as the cause of severe neonatal mortality. By examining the stunted progeny, it was discovered that the lethality was caused by hypercalcemia caused by high levels of $1,25(OH)_2D_3$ which could not be cleared from the circulation. In the late stages of pregnancy, pregnant knockout mice have very high levels of $1,25(OH)_2D_3$ which cannot be regulated by CYP24A1-mediated catabolism [3, 77]. In addition, continued administration of extrinsic $1,25(OH)_2D_3$ resulted in cortical tubular dilation, necrotic debris, and renal calcification observed in these mice, with excess of $1,25(OH)_2D_3$ that caused fatal calcium imbalance [3].

However, the surviving half of the breed is thought to have survived by regulating vitamin D in a different way. They were showing normal calcium and phosphate levels when they were fed standard rodent chow. The clearance of $1,25(OH)_2D_3$ remained poor in these mice, as seen by the absence of 24-hydroxylated metabolites as well as $1,25(OH)_2D$-26,23-lactone,

implying that vitamin D is regulated through inhibiting $1,25(OH)_2D_3$ synthesis rather than catabolism [3, 78]. The surviving pups had lower baseline circulating levels of $1,25(OH)_2D_3$ than their WT counterparts, implying that they are downregulating $1,25(OH)_2D_3$ production, allowing them to survive without major mineral homeostasis impairment [78].

When mice are bred from *Cyp24a1*-null mothers, the pups manifested high levels of $1,25(OH)_2D_3$. They also had osteoid accumulation and impaired bone mineralisation. Furthermore, the $24,25(OH)_2D_3$ administration during pregnancy to rescue the phenotype showed no improvement in bone abnormalities. The phenotype was rescued when crossed to VDR-ablated mice by preventing activity of the higher $1,25(OH)_2D_3$ levels during development [3].

On the other hand, albuminuria, hyperlipidemia, reduced circulating $25(OH)D_3$ and $24,25(OH)_2D_3$, low bone mineral density, and normal circulating $1,25(OH)_2D_3$ are observed after 8 weeks-of-age in transgenic rats where CYP24A1 is constitutively expressed. Also, the majority of the phenotype is thought to be caused by a change in renal function, although the cause is unknown. These findings suggest that $1,25(OH)_2D_3$ may have a role in vitamin D metabolism regulation [79, 80].

There is also evidence that $24,25(OH)_2D_3$ has an effect on chondrocytes during growth and fracture repair and itis probably affecting via a different mechanism than binding to the VDR receptor. Seo et al. (1997) found that circulating levels of $24,25(OH)_2D_3$ and CYP24A1 enzymatic activity increased in chicks by day 10 post-fracture and returned to basal levels by day 15, indicating that this metabolite and CYP24A1 enzymatic activity may be significant when damaged bones heal. They first found tritium-labeled $1,25(OH)_2D_3$ and $24,25(OH)_2D_3$ accumulation in growth plate cartilage [81]. However, no alteration of the growth plate cells

could be found in *Cyp24a1*-KO mice's growth plate chondrocytes [3]. They also discovered that tritium-labeled 24,25$(OH)_2D_3$ binds specifically to membrane portions of cells in chicks fracture callus [81]. When bones heal, however, 24,25$(OH)_2D_3$ and 1,25$(OH)_2D_3$ combination injected into the callus formation has a greater effect in bone renewal than 1,25$(OH)_2D_3$ solely [82].

Additional to those findings, it has been showed that the supplementation of the 24,25$(OH)_2D_3$ with the other D_3 metabolites during bone fracture repair had an improving effect on healing. They hypothesized that 24,25$(OH)_2D_3$ is required at a certain stage of chondrocyte development in the callus formation in chicks [83]. And also, it demonstrated that local injection of 24,25$(OH)_2D_3$ had an effect in rescuing rachitic cartilage and promoting fracture healing [84]. The callus membrane contained the putative binding protein/receptor with high and specific affinity to 24,25$(OH)_2D_3$, suggesting that 24,25$(OH)_2D_3$ might be acting via signal transduction response different from the regular steroid nuclear receptor [81].

The effect of 24,25$(OH)_2D_3$ on fracture repair was studied using *Cyp24a1*-null mice developed in the St-Arnaud's lab [3]. Their study showed that there is a significant delay on callus formation and healing in *Cyp24a1*-null mice compared to control littermates. Following the stabilized, transverse mid-diaphyseal fractures, at day 14 post-osteotomy, bone volume, force required to break the bone, and percentage of mineralized tissue were all reduced, and this could not be restored with 1,25$(OH)_2D_3$. However, the same group showed the improved histological appearance, biomechanical properties, and static histomorphometric index (BV/TV) when they were given daily injections of 24,25$(OH)_2D_3$ [4]. They also identified and cloned *Family with sequence similarity 57, member B2 (Fam57b2).* It encodes a protein that interacts with 24R,25$(OH)_2D_3$ in a saturable and stereo-specific way.

The *Fam57b* gene produces 3 isoforms through differential promoter usage [49]. Martineau et al. identified that cartilage and skin have the highest levels of expression of the second isoform, *Fam57b2.* Furthermore, the *FAM57B* gene was shown to have higher expression in patients with normal fractures compared to those with non-union fractures, indicating that it could play a role in fracture repair. Martineau et al. generated a mouse strain in which the *Fam57b* gene can be specifically inactivated in selected tissues. They bred *Fam57b*-floxed mice with Col2-Cre-transgenic mice to achieve chondrocyte-specific gene inactivation. Moreover, they identified the genetic pathway involving 24R,25$(OH)_2D_3$- induced, FAM57B2-dependent lactosylceramide (LacCer) production to rescue endochondral ossification during fracture repair using *Cyp24a1* KO mice [4]. LacCer are a class of glycosphyingolipids and the most abundant of the diosylceramides. In mammals, it acts as a metabolic branch point to produce many kinds of complex glycosphingolipids. It is thought to also control various aspects of cellular function [85]. Additionally LacCer-dependent signal transduction pathways have been identified [85]. Cell proliferation [86], adhesion [87, 88], apoptosis [89], and angiogenesis [90] have all been demonstrated to be influenced by these pathways. The St-Arnaud laboratory recently identified LacCer effect during bone healing [4].

Even though the *Cyp24a1*-null strain's feature and mimicking capacity of IIH disease were known, the locations of the mutations were unknown. Recently, 43 missense and deletion mutations of *CYP24A1* were described [91]. A small set of mutations in the *CYP24A1* gene comprising p. E143del, p.R396W, and p.L409S is detected in high frequency in the majority of patients. To find out whether a humanized mouse IIH model would also exhibit impaired fracture repair as *Cyp24a1*-KO strain, we generated the R396W mutated strain.

Initially the R396W knock-in embryonic stem cells were obtained from Cyagen and confirmed targeted clone was injected into C56Bl6/N blastocytes to develop the strain on this homogenous background.

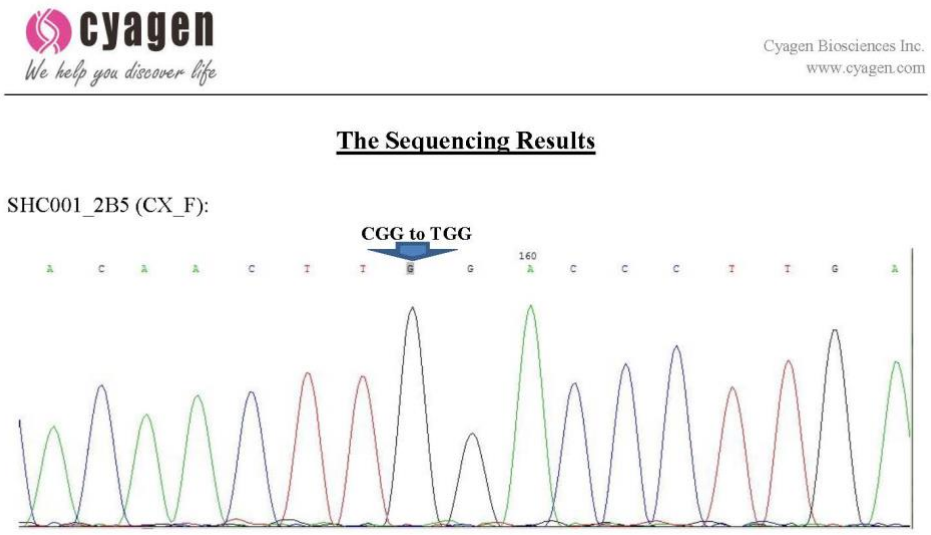

Figure 11 R396W mutation protein sequence alignments

The electrogram shows R396W missense mutation. Arginine (R) amino acid turns into Tryptophan (W) in position 396.

The R396W mutated on C56Bl6/N background showed higher 25(OH)D_3/24,25$(OH)_2D_3$ relativity (38.8) compared to WT littermates (6.7) as also seen in *Cyp24a1*-null mice. The strain showed a very low survival rate due to having lethally high concentrations of calcium. Also, the autopsy of non-surviving pups was showing nephrolithiasis. Finally, our laboratory crossed the R396W- C56Bl6/N strain with outbred CD1 mice. Eventually, the final generation, R396W-CD1, showed valid mimic of the IIH human condition with improved survival rates compared to C56Bl6/N backgrounded littermates.

Hypothesis

Based on our earlier work with the *Cyp24a1*-deficient model of IIH, we hypothesize that the humanized model sporting the R396W mutation will also exhibit impaired fracture repair. We will test this hypothesis through the following specific aims:

Aims

- Characterizing the fracture repair phenotype in the IIH mouse model.
- Determining the onset of the activity of $24,25(OH)_2D_3$ during fracture healing in IIH by setting new timepoints different than previous research.
- Outlining the biomechanical properties of the IIH mouse model.

Chapter II: Materials and Methods

2.1. Generation of R396W knock-in strain mutation and feeding

All animal procedures were reviewed and approved by the McGill Institutional Animal Care and Use Committee and followed the guidelines of the Canadian Council on Animal Care. Mice were kept in an environmentally controlled barrier animal facility with a 12-h light, 12-h dark cycle, and were fed mouse chow and water ad libitum.

The R396W knock-in ES cells were generated by Cyagen under contract. A confirmed targeted clone was injected into C57Bl6/N blastocysts to develop the strain on this homogeneous background. The R396W/R396W genotyped mice showed very low survival rate. More than 80% of the newborns did not survive past post-natal day 15. Homozygous mutants showed elevated doses of calcium levels and nephrolithiasis.

To improve survival, we crossed the strain with outbred CD1 mice. The R396W-CD1 pups all survived, and the strain is a valid mimic of the IIH human condition.

Eventually, we designed the study as 1) Generation of the mutant mice, 2) Performing the surgeries on their left tibias on the age of 3-months, 3) Harvesting the left tibias on day 10, day 14, and day 28 4) Testing the bones with TT on D14 and 28 or 3PBT and µCT scanning on D10. We finally tested 127 mice in total in order of 37, 49, and 41 mice in three different genotypes (Wild type [WT], heterozygous [+/R396W], homozygous mutant [R396W/R396W]), respectively. During surgeries, the right tibiae were protected and not included to the testing data.

2.2. Intramedullary Rodded Tibial Osteotomy

The surgical procedures were done as described in “Standard Procedure for Rodded Immobilized Fracture Surgery in the Mouse” of McGill University.

The intramedullary rodded immobilized open fracture surgery was performed on the left tibia at 2 and 3-months of age. The analyses of the fractured bones were performed on post-surgery days 10, 14 and 28 (D10, D14, D28).

Initially, the mice were weighted to determine the appropriate dosage of analgesic and to help monitor animal recovery. Then, the mice were injected subcutaneously with 1mg/kg body weight Buprenorphine (slow-release form, Chiron Computing Pharmacy, Inc.) thirty minutes prior to anesthesia. Mice were then anesthetised using oxygen and isoflurane gas and kept under anesthesia during the entire procedure. Following the anesthesia, a small amount of Natural Tear ointment was applied to each eye to prevent corneal drying during surgery. Subcutaneously 0.9% saline (0.2-0.5 ml/10g body weight) and Carprofen (Pfizer, NY, USA) (5ml/g body weight) were administered. The left leg was shaved from top of the leg to the foot to remove all fur surrounding the tibia and then washed with 70% alcohol and 2% chlorhexidine solutions, respectively. A 3mm vertical incision in the skin over the kneecap was made and the patellar ligament was exposed where a vertical medial parapatellar incision (approximately 1-1.5 mm in length) was made on the tibial plateau. A 26 G needle was vertically inserted through the incision into the tibial canal until the tip of the needle has reached the hollow canal, and through the needle, the internal wire guide of a 25 G BD spinal needle (Quincke 25 G 3” spinal needle, BD #450170, Franklin Lakes, USA) inserted into the canal and the 25 G needle was then removed while keeping the internal wire core guide in the tibial canal. The protruded part of the

wire core was cut, and a small 90° bend was made at its proximal part to avert puncture of the patellar ligament. The incision on the patellar ligament was then sutured. A mid-tibial shaft osteotomy was made using a bone scissor (Fine Science Tools #14082-09, Vancouver, Canada) by protecting the muscles around. Prior to closing the surgical site, 2-3 drops of Lidocaine 2% / Bupivacaine 0.5% (Wyeth, Ontario, Canada and Abbott Laboratories Ltd., Quebec, Canada, respectively) mixture were dropped to the site and incision then sutured with a single 6-0 vicryl suture (Johnson & Johnson, Skillman, USA) using horizontal mattress sutures as needed. Following the surgery, the mice were replaced into their clean cages on a heated pad and allowed to move around freely. The mice were then given subcutaneous injections of 5 ml/g body weight Carprofen at 24 hours and 48 hours post-surgery. The animals were closely monitored and any mice showing signs of severe pain, impaired mobility, bleeding, or swelling were euthanized.

All procedures were done under aseptic conditions in the procedure room of the animal facility at the Shriners Hospital for Children – Canada, Montreal, Quebec, Canada.

2.3 Sample Collection

The mice were sacrificed using isoflurane and CO_2 at D10, D14, and D28 post-surgery. The tibiae and calluses were dissected at the level of the knee and ankle. The intramedullary nail was carefully taken off. Tibiae and calluses were then harvested in PBS and directly transferred to test by µCT or kept in -20°C for further analyses via Torsion Test or 3-Point-Bending Test as planned.

2.4. Torsion Tests (TTs)

Torsion testing (twisting testing) was done to measure the biomechanical properties of the tibiae. The tibiae samples tested were D14 and D28 post-surgery. Initially, a small piece of tape covering the bottom of each disposable M6 fixture was used to hold the resin. The bone was embedded inside the M6 nuts with fast curing orthodontic acrylic resin mix (Ortho-Jet Liquid & Powder, Lang, USA) to rigidly constrain both ends. The bones were wrapped with 1X PBS-soaked gauze to maintain the hydration while the resin was hardening, usually overnight. The samples were inserted into holders attached to the micromechanical testing system (MACH-1 MA303-ART01-D v1 Lab Module, Biomomentum, Canada) as the proximal-end of the tibia was fixed and the distal-end was rotated.

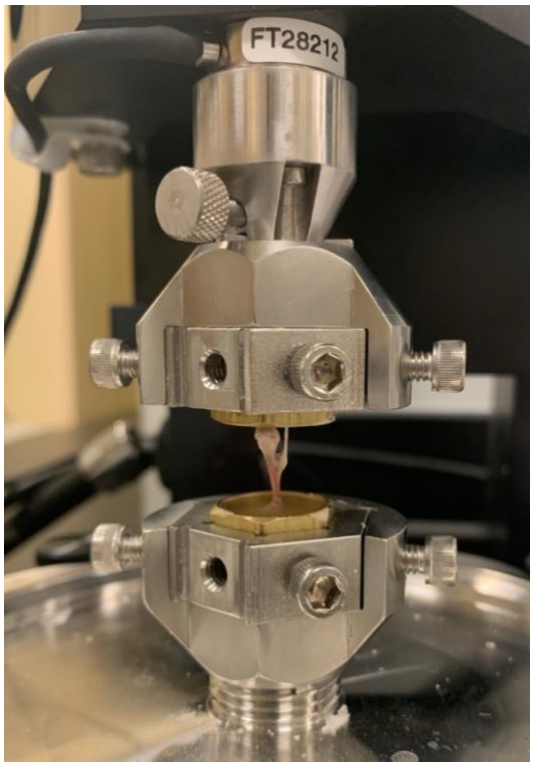

Figure 12 Torsional Testing Setup

The testing set with zero load and started from the theta position on the axis stage. Move relatives set as -360° amplitude and 0.5 deg/s velocity.

The biomechanical properties such as ultimate torque and torsional stiffness were acquired. Torsional stiffness (G) of the tibiae were measured from the slope of the linear portion of the curve and expressed in N-mm/deg (G $dM_t/d\theta_t$), and the torsional elasticity was measured as ultimate failure (W_t) [torque], named integral, and expressed in N-mm.deg ($W_t=\int_0^{\theta} M_t.d\theta$). in total 76 samples were tested (25 WT, 25 +/R396W, and 26 R396W/ R396W).

2.5. Micro-Computed Tomography

The Micro-Computed Tomography (μCT imaging were done to obtain the mineralized callus volume (percentage of bone volume to tissue volume [BV/TV]). To scan the tibias, mouse calluses and tibiae were harvested, on post operational day 10, discarded from soft tissue and stored in 1X PBS at -20°C until the analysis date. Right before the analysis, samples were dissolved, wrapped with 1X PBS-soaked gauze, and replaced to 0.6 ml tubes for imaging. The scanning of the tibias done by the desktop microtomographic imaging system (SkyScan 1272, Bruker AXS, Antwerp, Belgium).

The reconstruction was performed using 60kV, 166μA, 5-μm resolution, and a 0.5° rotation with 0.5-mm aluminum filter. The scanned samples were then moved to perform the 3-point bending tests (3PBTs) at the same day. The raw images were captured using NRecon software (Bruker). The trabecular volumes of interest (VOI) were defined and used to measure BV/TV. Trabecular regions set to cover all cancellous bone in metaphysis, within 2-mm-region slices. The manual contouring approach on a slice-by-slice basis was used for the callus

formational region of tibia. Tissue volume was set as a 20-mm^3 rectangular prism. And the analysing done using DataViewer and CTAn (both Bruker, Antwerp, Belgium). In total 44 samples were scanned (12 WT, 17 +/ R396W, and 15 R396W/ R396W)

2.6. Three Point Bending Tests (3PBTs)

3-Point bending testing is another biomechanical test that was used. The test was performed on tibiae isolated and then, scanned by µCT, using the Instron model 5943 single-column table frame machine. Bones were maintained in 1X PBS solution to maintain the hydration until testing. A downward bending load-sensing cell was applied on the widest part of the callus at 0.05 mm/s flow with a supporting distance 3 mm on each side of the callus which were held in place by holders spaced 6 millimetres apart. Raw output used for comparison is stiffness (N/mm) and strength (N). In total 45 samples were tested (12 WT, 19 +/ R396W, and 14 R396W/ R396W).

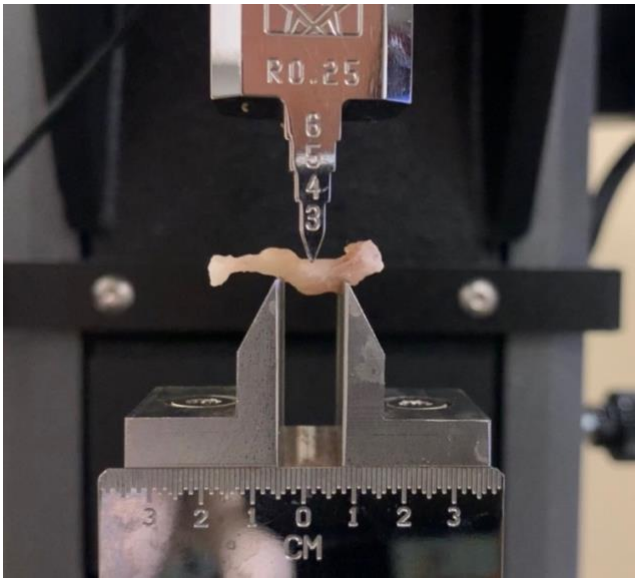

Figure 13. 3-PBT Setup

2.7. Statistical Analysis

The statistical analyses were done with GraphPad Prism (GraphPad Software). Statistical analyses were performed using a 2-tailed *t* test or 1-way ANOVA, followed by Bartlett's or, Bonferroni's post hoc test. The statistical significance threshold was set at a *P* value of less than 0.05.

Chapter III: Results

We used two separate methods to assess the biomechanical properties of the repair callus from mutant animals and littermate controls: torsion testing and the 3-point bending assay.

3.1. Torsion Testing

In a first set of experiments, torsion testing was performed. For this test, male and female mice from the three genotypes (Wild type [WT], heterozygous [+/R396W], homozygous mutant [R396W/R396W]) were analyzed. Mice were sacrificed and tibias were harvested at post-surgery D14 for female mice and D14 and D28 for male mice.

The results for male mice are presented first. A total of 25 male mice were analyzed at D14 (8 WT, 7 +/R396W, 10 R396W/R396W) and a total of 14 male mice (4 WT, 3 +/R396W, 7 R396W/R396W) were analyzed at D28.

We measured the ultimate torque parameter to assess the torsional elasticity of the callus tissue. At day 14 post-surgery, we did not see any significant differences among genotypes for this parameter (Figure 14, left). However, both heterozygous and homozygous male mice showed increase in ultimate torque at D28 post-surgery, and the difference were significant for the +/R396W genotype (Figure 14, right).

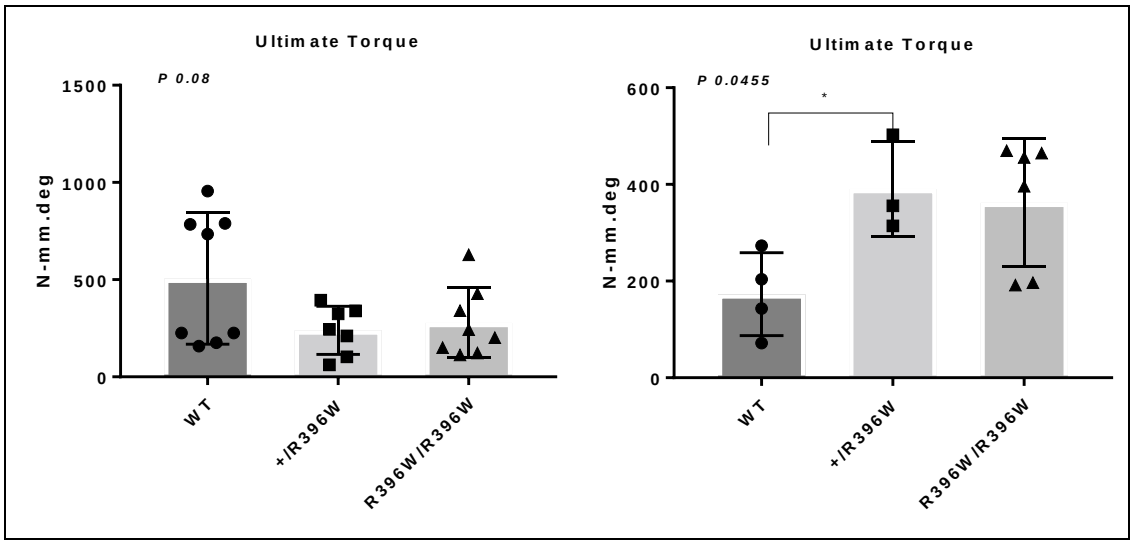

Figure 14 Ultimate Torque of male mice

The elasticity of the calluses was assessed by torsion test and calculated from the ultimate torque. **(Left)** Male mice on D14, did not show statistical significance. P>0.05, by one-way ANOVA followed by Bonferroni's post-test. **(Right)** Male mice on D28, showed significance between WT and +/R396W. *P 0.045, by one-way ANOVA followed by Bonferroni's post-test.

We next assessed the differences in the stiffness (slope) of the callus tissue among the different genotypes. At day 14 post-surgery, the WT data was too low to detect, and both heterozygous and homozygous mice showed an increase in callus stiffness as compared to WT male mice. The stiffness showed lowering trend compared to heterozygous littermates, but the difference was statistically non-significant. (Figure 15, left). However, when we analyzed the calluses at D28 post-surgery we noticed a significant decrease in stiffness for homozygous mutant mice as compared to their wild-type and heterozygous littermates (Figure 15, right).

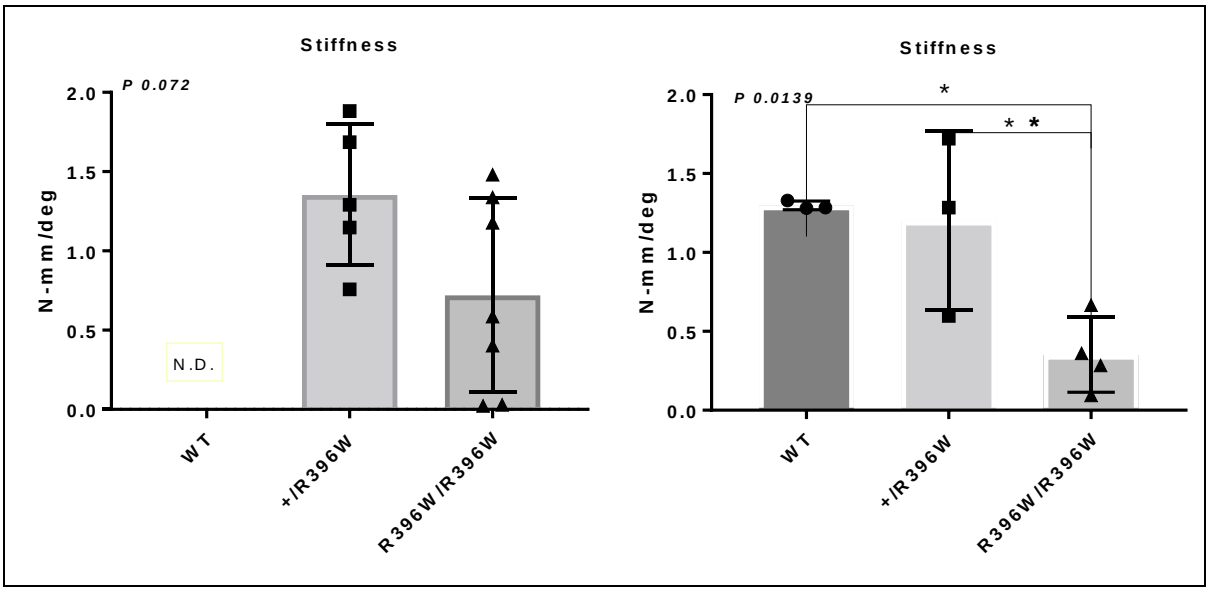

Figure 15 Stiffness of male mice

The stiffness of the calluses was assessed by torsion test and calculated from the slope. **(Left)** Male mice on D14, WT data was too low to detect (N.D. for Not Detectable). The difference between +/R396W and R396W/R396W was non-significant. P 0.072, by 2 -tailed t test. **(Right)** Male mice on D28, showed significance between mutant and both control genotypes. Median P 0.0139, *P 0,0250, **P 0.0415 by one-way ANOVA followed by Bonferroni's post-test.

For the female sex, 34 mice been used in total as 12 WT, 13 +/R396W and, 9 R396W/R396W. The bones were harvested at D14. The ultimate torque data were not statistically different between the genotypes (Figure 16). And the stiffness showed significant decrease towards mutant genotype and the difference were significant between heterozygous and mutant littermates (Figure 17).

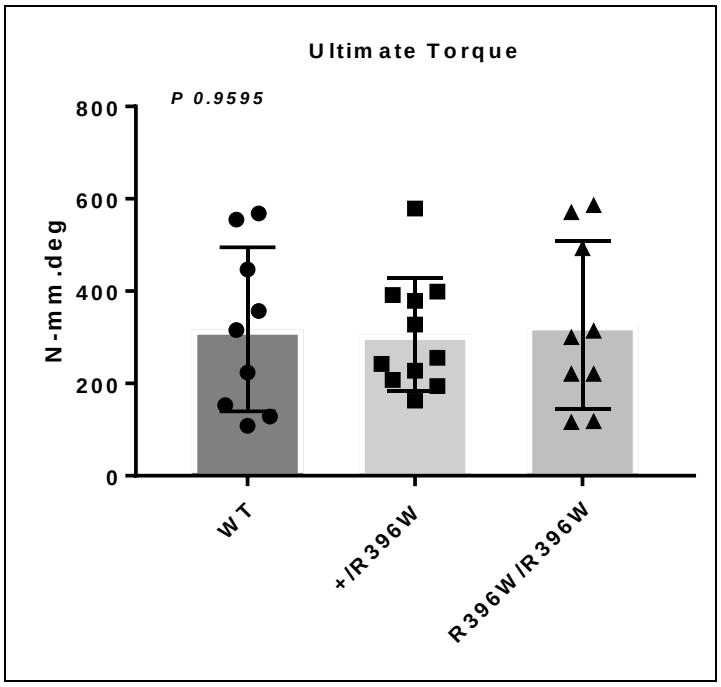

Figure 16 Ultimate Torque of D14-female mice

The elasticity of the calluses was assessed by torsion test and calculated from the ultimate torque. Female mice on D14, did not show significant differences. P>0.05, by one-way ANOVA followed by Bonferroni's post-test.

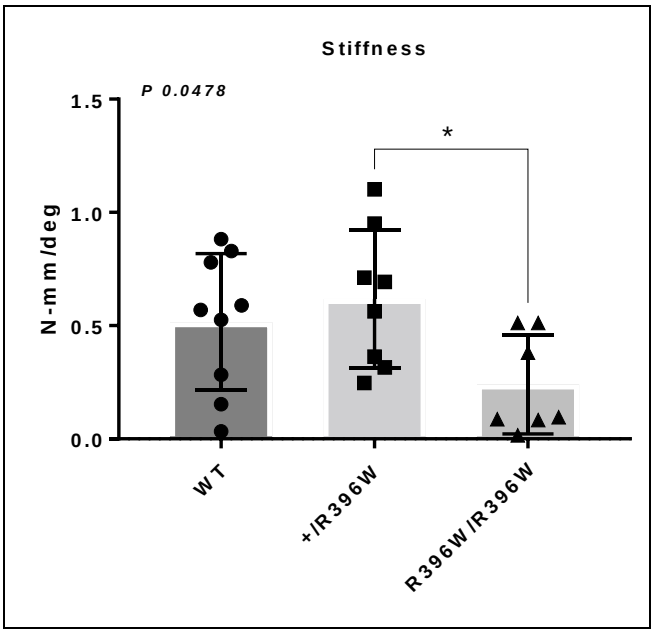

Figure 17 Stiffness of D14-female mice

The stiffness of the calluses was assessed by torsion test and calculated from the slope. Female mice on D14, showed statistical significance between +/R396W and R396W/ R396W. *P 0.0478, by one-way ANOVA followed by Bonferroni's post-test.

3.3. Micro-CT

We then analyzed the structural morphology of the callus tissue using micro-computed tomography imaging. We assessed the mineralized callus volume by calculating the percentage of bone volume to tissue volume (BV/TV) among the different genotypes. Males and females were sacrificed, and tibias were harvested on day 10 post-surgery.

A total of 34 male mice have been analyzed (10 WT, 10 +/R396W and, 14 R396W/R396W). The µCT analysis of calluses did not show a significance in mineralization between male littermates (Figure 18).

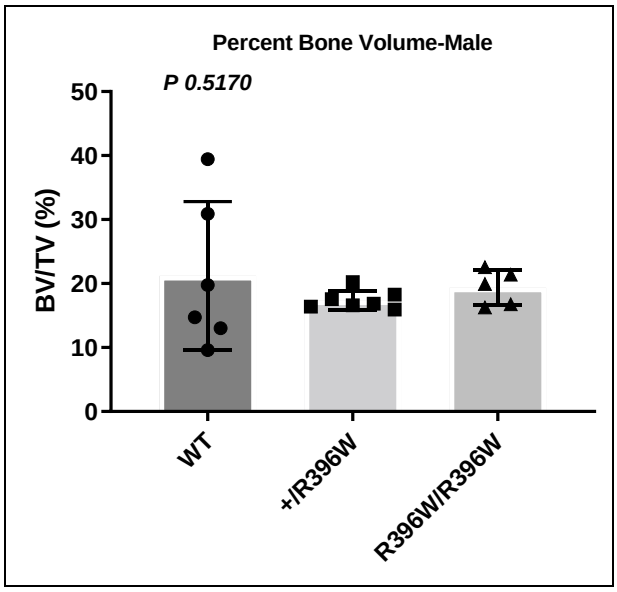

Figure 18 Percent bone volume of D10-male mice

The mineralized callus volume was assessed by µCT scanning and calculated as BV/TV. Male mice on D10 did not show significant differences between littermates. P>0.05, by one-way ANOVA followed by Bonferroni's post-test.

Similarly, a total of 24 female mice was analyzed (7 WT, 10 +/R396W and, 7 R396W/R396W). We measured significant differences in mineralized tissue among the genotypes (Figure 19).

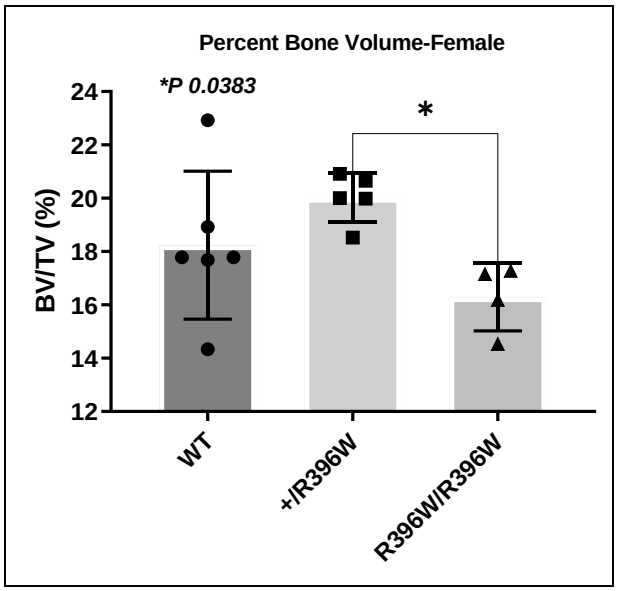

Figure 19 Percent bone volume of D10-female mice

The mineralized callus volume was assessed by µCT scanning and calculated as BV/TV. Female mice on D10 showed a significant difference between the +/R396W and R396W/ R396W littermates. *P 0.0383, by one-way ANOVA followed by Bonferroni's post-test.

3.2. Three-Point-Bending-Testing

To study the biomechanical properties of the callus tissue, the three-point bending test was performed following the µCT scanning. Females were sacrificed and tibias were harvested at post-surgical D10. Stiffness (N/mm) and strength (N) were measured.

For the male sex, 34 mice were used in total as 10 WT, 10 +/R396W and, 14 R396W/R396W. At D10 post-surgery, the analysis of the callus did not reveal any significant differences in stiffness among the different genotypes (Figure 20, left). We then analyzed the changes in the load at break parameter to assess the strength of the callus tissue. Interestingly, the analysis of heterozygous and homozygous calluses showed a significant decrease in load at break as compared to wild-type callus tissues (Figure 20, right).

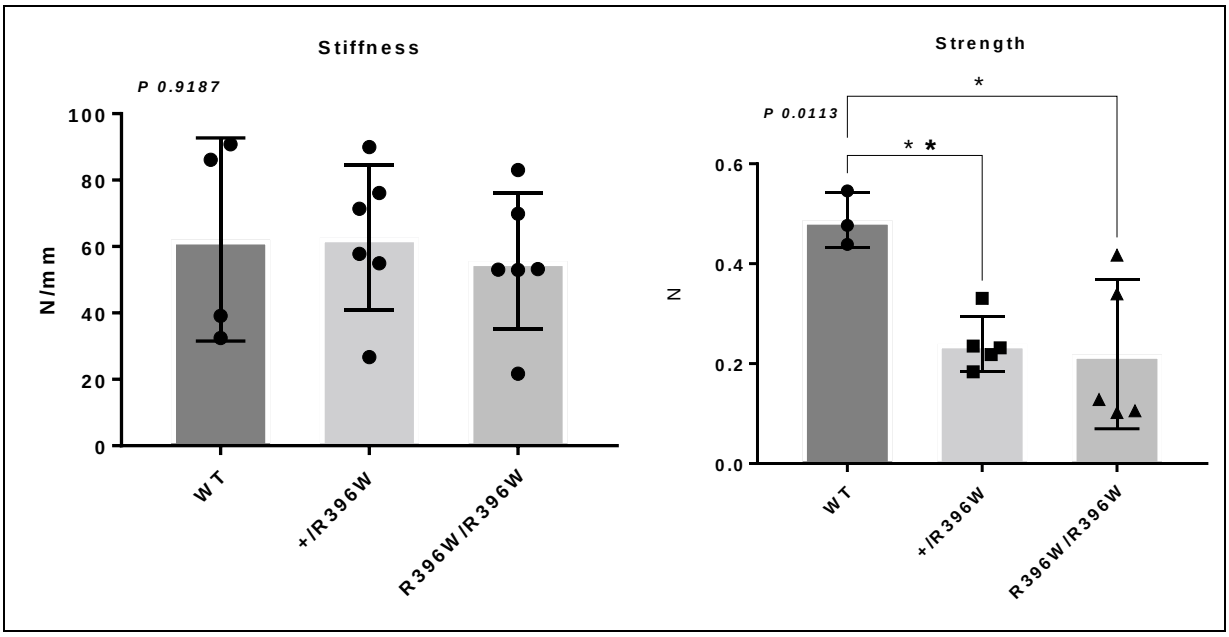

Figure 20 Stiffness and strength of male mice

The stiffness and strength of callus volume were assessed by 3PBTs and calculated from slope and load at break, respectively. **(Left)** The stiffness of male mice on D10 did not show differences between the littermates. P >0.05, by one-way ANOVA followed by Bonferroni's post-test. **(Right)** The strength of repair calluses from male mice on D10 showed a significant decrease as compared to wild-type callus tissues. *, P<0.05; **, P<0.01, by one-way ANOVA followed by Bonferroni's post-test.

A total of 24 female mice have been analyzed (7 WT, 10 +/R396W, and 7 R396W/R396W). The stiffness data were not significantly different between groups (Figure 21, left). As observed for the males, the strength data were significantly different compared to the wild-type genotype (Figure 21, right).

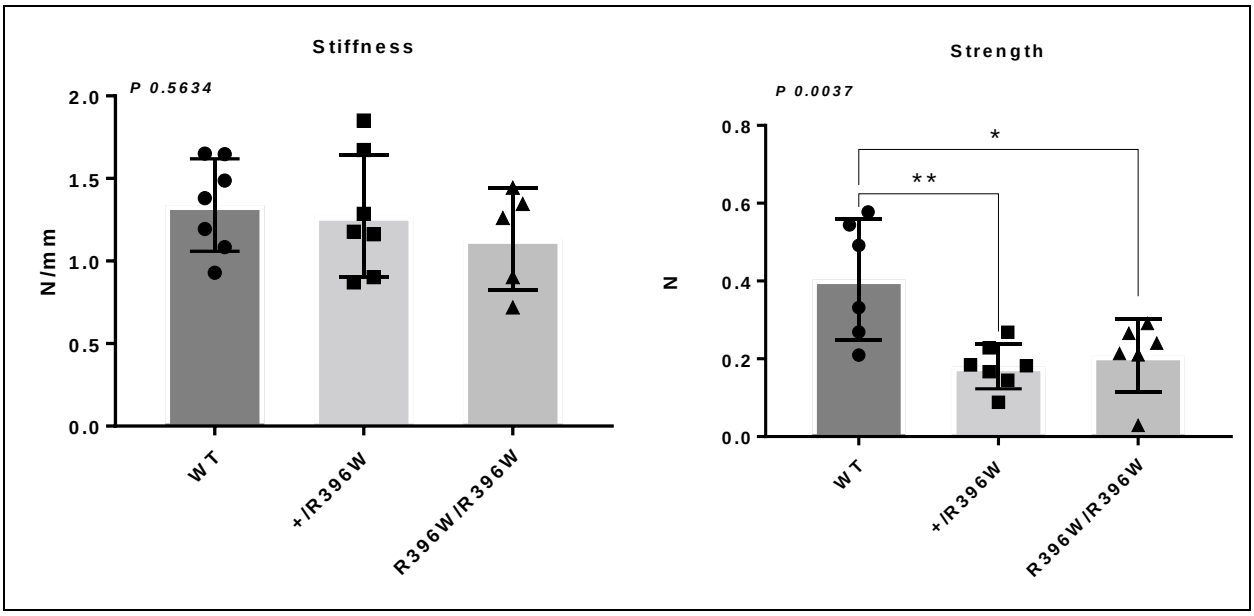

Figure 21 Stiffness and strength of female mice

The stiffness and strength of callus volume were assessed by 3PBTs and calculated from slope and load at break, respectively. **(Left)** The stiffness of female mice on D10 did not show differences between the littermates. P >0.05, by one-way ANOVA followed by Bonferroni's post-test. **(Right)** The strength of female mice on D10 showed a significant decrease in heterozygous and homozygous mutant genotypes (+/R396W and R396W/ R396W) compared to wild-type callus tissues Median P 0.0037, *P 0.0152, **P 0.0045, by one-way ANOVA followed by Bonferroni's post-test.

Taken together, the biomechanical analysis of the callus tissue of the different genotypes suggests a decrease in the mechanical strength towards the mutant (R396W/R396W) callus tissue as compared to wild-type calluses.

Chapter IV: Discussion

IIH is a rare genetic condition for which the genetic etiology remained unknown until 2011 when Schlingmann and coworkers identified the inactivation of CYP24A1 as a molecular basis [1]. The clinical manifestation of the disease is characterized by severe hypercalcemia, hypercalciuria, decreased PTH, nephrolithiasis, nephrocalcinosis with a predisposition to renal complications as well as dehydration, vomiting, and constipation [1]. In addition to *CYP24A1* mutations, the Schlingmann group identified *SLC34A1* genetic variants as the cause of IIH forms with some clinical differences [76]. These results suggest that a complete diagnostic of patients presenting with IIH symptoms should include genetic testing together with assessment of the 25(OH)D_3-to-24,25(OH)$_2D_3$ ratio [76, 92].

Biallelic mutations causing complete loss-of-function of the CYP24A1 activity have been demonstrated previously. As a result, hypervitaminosis D occurs and that leads to increased intestinal absorption of calcium and symptomatic hypercalcemia.

Even though it was hypothesized that *CYP24A1* mutations were leading to IIH condition, the locations of the mutations were unknown. Recently, 43 missense and deletion mutations of *CYP24A1* were described [91]. A small set of mutations in the *CYP24A1* gene comprising p.E143del, p.R396W, and p.L409S is detected in high frequency in the majority of patients. Our team previously showed that *Cyp24a1*-null mice with a deletion of exons 9-10 replaced by a PGKneo selection cassette, mimicked the disease IIH [4]. It also displayed impaired callus formation during the endochondral phase of fracture repair. They also observed that treatment with 24,25(OH)$_2D_3$ was able to rescue callus size and stiffness, but 1,25(OH)$_2D_3$ treatment was ineffective to correct the impaired bone fracture healing.

Based on previous findings, we hypothesized that a humanized model of IIH in genetically modified mice harboring a knock-in R396W mutation will exhibit impaired fracture repair. We predicted that this mutation would cause a slower healing rate and weaker bone biomechanical properties on the mutant R396W/R396W genotype compared to WT by affecting production of the $24,25(OH)_2D_3$ metabolite. To test our hypothesis, we designed the proper research model. We initially obtained the R396W knock-in ES cells from Cyagen under contract and finally generated the R396W-CD1 mice strain. This strain is a phenocopy of the IIH human condition (unpublished data from the St-Arnaud laboratory). We then performed a bone fracture healing study design based on experiments previously done by the St-Arnaud laboratory to assess whether the strain has impaired fracture repair. We performed the rodded tibial osteotomy on 12-weeks-of-age mice and harvested the healing tibial bones at D10, D14, and D28.

In the current study, in addition to the previous biomechanical endpoints, we added a new technique to obtain material properties of the callus tissue post-surgery, i.e. torsion testing.

A torsion test ideally examines bone behavior under shear stress, which is also important in vivo. The callus diameter has a significant impact on the strength when calculating biomechanical properties under torsion, with the cross-sectional moment of inertia corresponding to the fourth magnitude of the radius diameter. As a result, even slight changes in callus size have a significant impact on the bone's ability to bear torsional pressures [93]. Based on these parameters, one would expect the torsion breaking strength of the larger calluses to be significantly higher.

Our findings did not entirely agree with these notions and torsional testing generated some discordant results. For example, the callus elasticity (integral) from the homozygous mutant animals was higher than their WT littermates at D28 post-surgery in male mice. Also, the

stiffness levels were higher in heterozygous and mutant male animals than WT mice at D14 post-surgery.

The cause of these disparities appears technical. Stiffness of male WT calluses was not detectable at D14 (Figure 15, left panel). When results from heterozygous animals were compared to homozygous mutants, the lower stiffness measured in mutants showed lowering trend even though the difference was not significant.

Torsion stresses the entire bone between the fixation points equally, causing the weakest component of the bone to break first. Newly generated calluses continue into previously unfractured bone sections with biomechanical qualities that are very similar to native bone. It was not possible to isolate the calluses and assess their torsion strength with this test since some calluses were stronger than non-fractured regions of the bone (Figure 22). Also, when we looked through the literature, we found out that another research group was faced with a similar problem (Figure 23) [94]. In the research design of Bosemark et al., they performed the torsion testing following the rodded femoral osteotomy on rat's femur. They harvested the rats' femurs on post-operational week 6 and implemented biomechanical testing such as 3-PBT and TT. They were successful to measure the properties of the callus formation on 3-PBT but, during TT (twisting) some of their samples were breaking from points other than callus area [94].

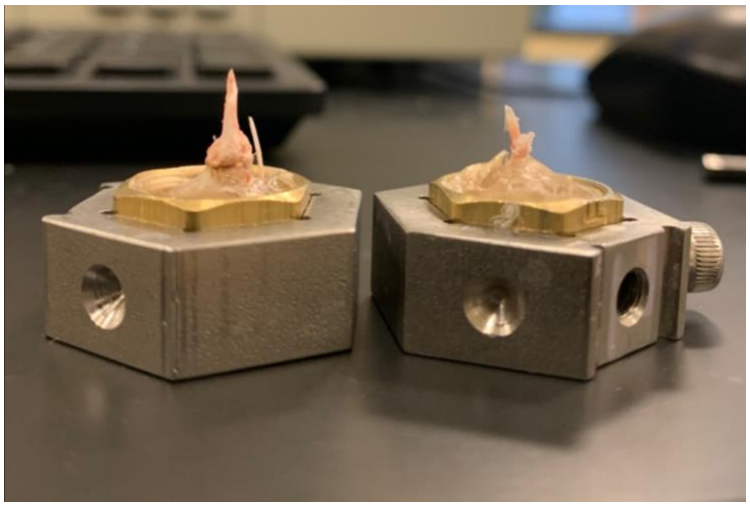

Figure 22 TT- Bone breaks from the weakest point other than callus

During TT, numerous tibias broke from the weakest point regardless of their sex and genotype. Thus, the data were obtained from the bone sections other than the callus formation. Meaning that, biomechanical properties of callus were not being tested.

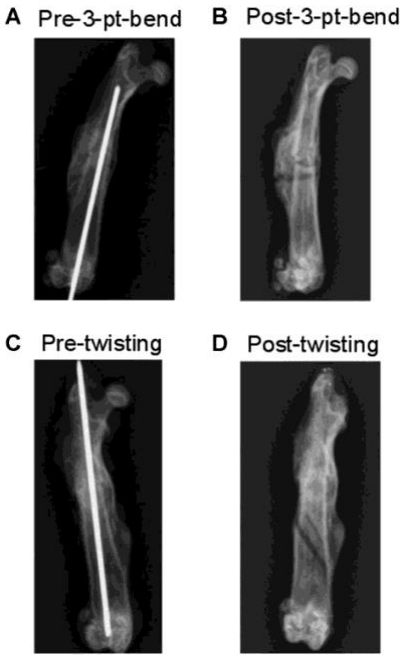

Figure 23. Pre- and post-twisting test.

The figure shows the rat femurs on post-surgery week 6. The intramedullary rod can be seen on pre-twisting images (**A and C)**. As it shows the breaking line is on callus formation in post-3PBT image (**B)**, but it is in below callus, towards to distal end in post-twisting (**D**). Figure adapted from Bosemark (2014) [94],with permission.

So even though we estimated that torsion testing would be preferable, we found that there are technical limitations to analyzing the samples as seen in our and Bosemark and coworkers research [94]. This issue might be overcome by changing the bone harvesting days to an earlier time point than 14 days. So, the callus might be the weakest point in the sample.

We then prepared another cohort to test the biomechanical properties of our R396W-CD1 strain with more conventional assays, µCT scanning and 3PBTs. After performing the same intramedullary rodded fracture surgery, we followed the same procedure as previously done in our lab [4] except we changed the timeline from post-operational D14 to D10 to additionally determine the onset of the activity of $24,25(OH)_2D_3$ during fracture healing in IIH.

Our µCT scanning results showed similar outcomes as Martineau et al. obtained [4]. R396W-CD1 mouse strain showed significantly lower sizes of mineralized callus volume (BV/TV) in female mice compared to heterozygous littermates, and it showed a lowering trend in male sex towards the mutant genotype.

3PBTs results were also having similarities with previous findings [4]. The stiffness did not show significance in both sexes although they were having a lowering rate towards the mutant strain. The strength data (load at break), on the other hand, showed a significant decrease in R396W-mutated mice in both sexes.

Chapter V: Conclusions and Future Directions

Our study aimed to characterize fracture repair in a humanized IIH mouse model and outline the biomechanical properties of the IIH mouse model.

As R396W mutations are among the most common types of mutations associated with *CYP24A1* polymorphisms, we expected to see impaired fracture repair as seen in Martineau et.al research [4]. Our data supported our hypothesis that the mutant littermates would exhibit impaired fracture repair compared to WT littermates. These outcomes show that the humanized preclinical model of IIH has similar phenotypic manifestations to the original *Cyp24a1*-null mice which sported a deletion of exons 9-10, insertion of a selection cassette in the opposite transcriptional orientation and did not express the *Cyp24a1* transcript [3].

Previously, it has been shown that optimal bone fracture repair requires $24,25(OH)_2D_3$ and its effector molecule FAM57B2 [4]. In our study, by changing the analysis timepoints from D14 to D10, we observed similar outcomes at the level of biomechanical properties. This suggests that $24,25(OH)_2D_3$ has an earlier role during fracture repair. This has an important impact on bone health and the healing rate in both healthy and ill individuals, as the literature points to high rates of immobility and fatality in adults with long bone fractures. Also, it is known that IIH patients have imbalanced vitamin-mineral homeostasis and lower bone mass compared to unaffected individuals [74]. Taken together, our results raise the question as to whether $24,25(OH)_2D_3$ supplementation as part of treatment would help achieve complete fracture healing or not. Our mouse model is promising to be used in such research in the future.

During our research, even though we estimated that torsion testing would be preferable, we found that there are technical limitations to analyzing the samples. It showed that using torsion testing for fracture healing research should be considered carefully. Setting an earlier

timepoint might help to overcome the issues. Also, performing histological analysis in addition to the methods that we have used would help to further characterize the phenotype of R396W mice.

Another limitation of our work is the lack of histological scanning. We suggest applying histological scanning to the future researches.

Based on our work and previous findings in this regard, it has been shown that $24,25(OH)_2D_3$ has a significant role during fracture repair. However, it is still unknown whether the effect of $24,25(OH)_2D_3$ on bone regeneration is dependent exclusively on chondrocytes or involves some other cell type. To answer this question, a chondrocyte-specific mouse model is being generated to further investigate this issue.

Furthermore, in patients with IIH, it should be possible to study fracture repair in a prospective way following the fracture, by taking high-resolution peripheral quantitative computed tomography (HR-pQCT) images at intervals to find evidence of reduced callus size. Finite element modeling (FEM) could predict that the biomechanical parameters of affected bones are weaker. This would support the use of $24,25(OH)_2D_3$ as therapy for treating fractures.

As every human being is unique, so are their diseases. Mapping the subtypes of genetic diseases could help the development of personalized medicine approaches as new treatments. Identifying the subtypes and applying specific treatments may have a big impact on enhancing the life quality of patients and minimizing the healthcare expenses.

Chapter VI: References

1. Schlingmann, K.P., et al., *Mutations in CYP24A1 and idiopathic infantile hypercalcemia.* N Engl J Med, 2011. **365**(5): p. 410-21.
2. Feldman, D., J.W. Pike, and R. Bouillon, *Vitamin D*. Fourth edition. ed. 2018, London, United Kingdom ;: Academic Press. 2 volumes.
3. St-Arnaud, R., et al., *Deficient mineralization of intramembranous bone in vitamin D-24-hydroxylase-ablated mice is due to elevated 1,25-dihydroxyvitamin D and not to the absence of 24,25-dihydroxyvitamin D.* Endocrinology, 2000. **141**(7): p. 2658-66.
4. Martineau, C., et al., *Optimal bone fracture repair requires 24R,25-dihydroxyvitamin D3 and its effector molecule FAM57B2.* J Clin Invest, 2018. **128**(8): p. 3546-3557.
5. Clarke, B., *Normal bone anatomy and physiology.* Clin J Am Soc Nephrol, 2008. **3 Suppl 3**: p. S131-9.
6. Taichman, R.S., *Blood and bone: two tissues whose fates are intertwined to create the hematopoietic stem-cell niche.* Blood, 2005. **105**(7): p. 2631-9.
7. Zhou, R., et al., *Endocrine role of bone in the regulation of energy metabolism.* Bone Res, 2021. **9**(1): p. 25.
8. Treuting, P., S. Dintzis, and K.S. Montine, *Comparative Anatomy and Histology*. 2012.
9. Roothaer, X., *Multi-scale study of the mechanical behaviour of bearing and bone-bearing bones : towards personalization of FE human models*. 2019.
10. Florencio-Silva, R., et al., *Biology of Bone Tissue: Structure, Function, and Factors That Influence Bone Cells.* Biomed Res Int, 2015. **2015**: p. 421746.
11. Mulari, M., J. Vääräniemi, and H.K. Väänänen, *Intracellular membrane trafficking in bone resorbing osteoclasts.* Microscopy research and technique, 2003. **61**(6): p. 496-503.

12. Percival, C.J. and J.T. Richtsmeier, *Angiogenesis and intramembranous osteogenesis.* Dev Dyn, 2013. **242**(8): p. 909-22.

13. Brighton, C.T. and R.M. Hunt, *Early histological and ultrastructural changes in medullary fracture callus.* J Bone Joint Surg Am, 1991. **73**(6): p. 832-47.

14. Aaron, R.K., et al., *Clinical biophysics: the promotion of skeletal repair by physical forces.* Ann N Y Acad Sci, 2006. **1068**: p. 513-31.

15. Cserjesi, P., et al., *Scleraxis: a basic helix-loop-helix protein that prefigures skeletal formation during mouse embryogenesis.* Development, 1995. **121**(4): p. 1099-110.

16. Šošić, D., et al., *Regulation of paraxis expression and somite formation by ectoderm- and neural tube-derived signals.* Dev Biol, 1997. **185**(2): p. 229-43.

17. Mackie, E.J., et al., *Endochondral ossification: how cartilage is converted into bone in the developing skeleton.* Int J Biochem Cell Biol, 2008. **40**(1): p. 46-62.

18. White, A. and G. Wallis, *Endochondral ossification: a delicate balance between growth and mineralisation.* Curr Biol, 2001. **11**(15): p. R589-91.

19. Carballo, C.B., et al., *Basic science of articular cartilage.* Clinics in sports medicine, 2017. **36**(3): p. 413-425.

20. Chen, H., et al., *Molecular Mechanisms of Chondrocyte Proliferation and Differentiation.* Frontiers in Cell and Developmental Biology, 2021. **9**.

21. Jiang, Q., et al., *Antxr1, Which is a Target of Runx2, Regulates Chondrocyte Proliferation and Apoptosis.* Int J Mol Sci, 2020. **21**(7).

22. Rim, Y.A., Y. Nam, and J.H. Ju, *The Role of Chondrocyte Hypertrophy and Senescence in Osteoarthritis Initiation and Progression.* Int J Mol Sci, 2020. **21**(7).

23. Charlier, E., et al., *Chondrocyte dedifferentiation and osteoarthritis (OA).* Biochem Pharmacol, 2019. **165**: p. 49-65.

24. Parreno, J., et al., *Interplay between cytoskeletal polymerization and the chondrogenic phenotype in chondrocytes passaged in monolayer culture.* J Anat, 2017. **230**(2): p. 234-248.

25. Richter, D.L., et al., *Knee articular cartilage repair and restoration techniques: a review of the literature.* Sports health, 2016. **8**(2): p. 153-160.

26. Kozhemyakina, E., A.B. Lassar, and E. Zelzer, *A pathway to bone: signaling molecules and transcription factors involved in chondrocyte development and maturation.* Development, 2015. **142**(5): p. 817-831.

27. Guntur, A.R. and C.J. Rosen, *Bone as an endocrine organ.* Endocrine practice : official journal of the American College of Endocrinology and the American Association of Clinical Endocrinologists, 2012. **18**(5): p. 758-762.

28. Karsenty, G. and E.F. Wagner, *Reaching a genetic and molecular understanding of skeletal development.* Dev Cell, 2002. **2**(4): p. 389-406.

29. Yoda, K., *Bone as an endocrine organ: diabetic bone disease as a cause of endocrine disorder via osteocalcin, FGF23 secreted from osteocyte/osteoblast*, in *Musculoskeletal Disease Associated with Diabetes Mellitus*. 2016, Springer. p. 113-123.

30. Winkler, D.G., et al., *Osteocyte control of bone formation via sclerostin, a novel BMP antagonist.* EMBO J, 2003. **22**(23): p. 6267-76.

31. Shimada, T., et al., *Targeted ablation of Fgf23 demonstrates an essential physiological role of FGF23 in phosphate and vitamin D metabolism.* J Clin Invest, 2004. **113**(4): p. 561-8.

32. Han, Y., et al., *Paracrine and endocrine actions of bone—the functions of secretory proteins from osteoblasts, osteocytes, and osteoclasts.* Bone Research, 2018. **6**(1): p. 16.

33. Ducy, P., et al., *Increased bone formation in osteocalcin-deficient mice.* Nature, 1996. **382**(6590): p. 448-52.

34. Otani, T., et al., *Signaling pathway for adiponectin expression in adipocytes by osteocalcin.* Cell Signal, 2015. **27**(3): p. 532-44.

35. Mosialou, I., et al., *MC4R-dependent suppression of appetite by bone-derived lipocalin 2.* Nature, 2017. **543**(7645): p. 385-390.

36. Batoon, L., et al., *Osteomacs and Bone Regeneration.* Curr Osteoporos Rep, 2017. **15**(4): p. 385-395.

37. Einhorn, T.A. and L.C. Gerstenfeld, *Fracture healing: mechanisms and interventions.* Nature Reviews Rheumatology, 2015. **11**(1): p. 45-54.

38. Giannoudis, P.V., T.A. Einhorn, and D. Marsh, *Fracture healing: the diamond concept.* Injury, 2007. **38 Suppl 4**: p. S3-6.

39. Majidinia, M., A. Sadeghpour, and B. Yousefi, *The roles of signaling pathways in bone repair and regeneration.* J Cell Physiol, 2018. **233**(4): p. 2937-2948.

40. Gomez-Barrena, E., et al., *Bone fracture healing: cell therapy in delayed unions and nonunions.* Bone, 2015. **70**: p. 93-101.

41. Walters, G., I. Pountos, and P.V. Giannoudis, *The cytokines and micro-environment of fracture haematoma: Current evidence.* J Tissue Eng Regen Med, 2018. **12**(3): p. e1662-e1677.

42. Zhou, F.H., et al., *TNF-alpha mediates p38 MAP kinase activation and negatively regulates bone formation at the injured growth plate in rats.* J Bone Miner Res, 2006. **21**(7): p. 1075-88.

43. Schindeler, A. and D.G. Little, *Ras-MAPK signaling in osteogenic differentiation: friend or foe?* J Bone Miner Res, 2006. **21**(9): p. 1331-8.

44. Krishnan, V., H.U. Bryant, and O.A. Macdougald, *Regulation of bone mass by Wnt signaling.* J Clin Invest, 2006. **116**(5): p. 1202-9.

45. Hilton, M.J., et al., *Notch signaling maintains bone marrow mesenchymal progenitors by suppressing osteoblast differentiation.* Nat Med, 2008. **14**(3): p. 306-14.

46. Zhu, F., M.T. Sweetwyne, and K.D. Hankenson, *PKCdelta is required for Jagged-1 induction of human mesenchymal stem cell osteogenic differentiation.* Stem Cells, 2013. **31**(6): p. 1181-92.

47. Carreira, A.C., et al., *Bone morphogenetic proteins: facts, challenges, and future perspectives.* J Dent Res, 2014. **93**(4): p. 335-45.

48. Shah, A.D., et al., *Maternal Hypercalcemia Due to Failure of 1,25-Dihydroxyvitamin-D3 Catabolism in a Patient With CYP24A1 Mutations.* J Clin Endocrinol Metab, 2015. **100**(8): p. 2832-6.

49. Arvidson, K., et al., *Bone regeneration and stem cells.* J Cell Mol Med, 2011. **15**(4): p. 718-46.

50. Ornitz, D.M. and P.J. Marie, *FGF signaling pathways in endochondral and intramembranous bone development and human genetic disease.* Genes Dev, 2002. **16**(12): p. 1446-65.

51. Yun, Y.R., et al., *Fibroblast growth factors: biology, function, and application for tissue regeneration.* J Tissue Eng, 2010. **2010**: p. 218142.

52. Holick, M.F., *Vitamin D deficiency.* N Engl J Med, 2007. **357**(3): p. 266-81.

53. Calvo, M.S., S.J. Whiting, and C.N. Barton, *Vitamin D fortification in the United States and Canada: current status and data needs.* Am J Clin Nutr, 2004. **80**(6 Suppl): p. 1710S-6S.

54. Webb, A.R., L. Kline, and M.F. Holick, *Influence of season and latitude on the cutaneous synthesis of vitamin D3: exposure to winter sunlight in Boston and Edmonton will not promote vitamin D3 synthesis in human skin.* J Clin Endocrinol Metab, 1988. **67**(2): p. 373-8.

55. Deeb, K.K., D.L. Trump, and C.S. Johnson, *Vitamin D signalling pathways in cancer: potential for anticancer therapeutics.* Nat Rev Cancer, 2007. **7**(9): p. 684-700.

56. Heaney, R.P., *Vitamin D in health and disease.* Clin J Am Soc Nephrol, 2008. **3**(5): p. 1535-41.

57. Jablonski, N.G. and G. Chaplin, *The evolution of human skin coloration.* J Hum Evol, 2000. **39**(1): p. 57-106.

58. Movassaghi, M., et al., *Vitamin D levels in Smith-Lemli-Opitz syndrome.* American Journal of Medical Genetics Part A, 2017. **173**(10): p. 2577-2583.

59. Molin, A., et al., *Vitamin D–Dependent Rickets Type 1B (25-Hydroxylase Deficiency): A Rare Condition or a Misdiagnosed Condition?* Journal of Bone and Mineral Research, 2017. **32**(9): p. 1893-1899.

60. Fraser, D., et al., *Pathogenesis of hereditary vitamin-D-dependent rickets: an inborn error of vitamin D metabolism involving defective conversion of 25-hydroxyvitamin D to*

1α, 25-dihydroxyvitamin D. New England Journal of Medicine, 1973. **289**(16): p. 817-822.

61. Jones, G., D.E. Prosser, and M. Kaufmann, *25-Hydroxyvitamin D-24-hydroxylase (CYP24A1): its important role in the degradation of vitamin D.* Archives of biochemistry and biophysics, 2012. **523**(1): p. 9-18.

62. Plum, L.A. and H.F. DeLuca, *Vitamin D, disease and therapeutic opportunities.* Nat Rev Drug Discov, 2010. **9**(12): p. 941-55.

63. Kerry, D.M., et al., *Transcriptional synergism between vitamin D-responsive elements in the rat 25-hydroxyvitamin D3 24-hydroxylase (CYP24) promoter.* J Biol Chem, 1996. **271**(47): p. 29715-21.

64. Kumar, R., et al., *Systematic characterisation of the rat and human CYP24A1 promoter.* Mol Cell Endocrinol, 2010. **325**(1-2): p. 46-53.

65. Pike, J.W. and M.B. Meyer, *Regulation of mouse Cyp24a1 expression via promoter-proximal and downstream-distal enhancers highlights new concepts of 1,25-dihydroxyvitamin D(3) action.* Arch Biochem Biophys, 2012. **523**(1): p. 2-8.

66. Beckman, M.J., et al., *Human 25-hydroxyvitamin D3-24-hydroxylase, a multicatalytic enzyme.* Biochemistry, 1996. **35**(25): p. 8465-72.

67. Horst, R.L., et al., *Impaired 24,25-dihydroxyvitamin D production in anephric human and pig.* J Clin Invest, 1981. **67**(1): p. 274-80.

68. Shigematsu, T., et al., *Human parathyroid hormone inhibits renal 24-hydroxylase activity of 25-hydroxyvitamin D3 by a mechanism involving adenosine 3',5'-monophosphate in rats.* Endocrinology, 1986. **118**(4): p. 1583-9.

69. Shinki, T., et al., *Parathyroid hormone inhibits 25-hydroxyvitamin D3-24-hydroxylase mRNA expression stimulated by 1 alpha,25-dihydroxyvitamin D3 in rat kidney but not in intestine.* J Biol Chem, 1992. **267**(19): p. 13757-62.

70. Henry, H.L., *The 25(OH)D(3)/1alpha,25(OH)(2)D(3)-24R-hydroxylase: a catabolic or biosynthetic enzyme?* Steroids, 2001. **66**(3-5): p. 391-8.

71. Lightwood, R. and T. Stapleton, *Idiopathic hypercalcaemia in infants.* Lancet, 1953. **265**(6779): p. 255-6.

72. Stapleton, T., W.B. Macdonald, and R. Lightwood, *The pathogenesis of idiopathic hypercalcemia in infancy.* Am J Clin Nutr, 1957. **5**(5): p. 533-42.

73. Gut, J. and S. Kutilek, *Idiopathic infantile hypercalcaemia in 5-month old girl.* Prague Med Rep, 2011. **112**(2): p. 124-31.

74. Ferraro, P.M., et al., *A novel CYP24A1 genotype associated to a clinical picture of hypercalcemia, nephrolithiasis and low bone mass.* Urolithiasis, 2017. **45**(3): p. 291-294.

75. Figueres, M.L., et al., *Kidney function and influence of sunlight exposure in patients with impaired 24-hydroxylation of vitamin D due to CYP24A1 mutations.* Am J Kidney Dis, 2015. **65**(1): p. 122-6.

76. Schlingmann, K.P., et al., *Autosomal-Recessive Mutations in SLC34A1 Encoding Sodium-Phosphate Cotransporter 2A Cause Idiopathic Infantile Hypercalcemia.* J Am Soc Nephrol, 2016. **27**(2): p. 604-14.

77. Kovacs, C.S. and H.M. Kronenberg, *Maternal-fetal calcium and bone metabolism during pregnancy, puerperium, and lactation.* Endocr Rev, 1997. **18**(6): p. 832-72.

78. Masuda, S., et al., *Altered pharmacokinetics of 1alpha,25-dihydroxyvitamin D3 and 25-hydroxyvitamin D3 in the blood and tissues of the 25-hydroxyvitamin D-24-hydroxylase (Cyp24a1) null mouse.* Endocrinology, 2005. **146**(2): p. 825-34.

79. Hosogane, N., et al., *Mechanisms for the reduction of 24,25-dihydroxyvitamin D3 levels and bone mass in 24-hydroxylase transgenic rats.* FASEB J, 2003. **17**(6): p. 737-9.

80. Kasuga, H., et al., *Characterization of transgenic rats constitutively expressing vitamin D-24-hydroxylase gene.* Biochem Biophys Res Commun, 2002. **297**(5): p. 1332-8.

81. Seo, E.G., A. Kato, and A.W. Norman, *Evidence for a 24R,25(OH)2-vitamin D3 receptor/binding protein in a membrane fraction isolated from a chick tibial fracture-healing callus.* Biochem Biophys Res Commun, 1996. **225**(1): p. 203-8.

82. Kato, A., et al., *Studies on 24R,25-dihydroxyvitamin D3: evidence for a nonnuclear membrane receptor in the chick tibial fracture-healing callus.* Bone, 1998. **23**(2): p. 141-6.

83. Seo, E.G., T.A. Einhorn, and A.W. Norman, *24R,25-dihydroxyvitamin D3: an essential vitamin D3 metabolite for both normal bone integrity and healing of tibial fracture in chicks.* Endocrinology, 1997. **138**(9): p. 3864-72.

84. Lidor, C., et al., *Healing of rachitic lesions in chicks by 24R,25-dihydroxycholecalciferol administered locally into bone.* J Bone Miner Res, 1987. **2**(2): p. 91-8.

85. Chatterjee, S. and A. Pandey, *The Yin and Yang of lactosylceramide metabolism: implications in cell function.* Biochim Biophys Acta, 2008. **1780**(3): p. 370-82.

86. Bhunia, A.K., et al., *Lactosylceramide Stimulates Ras-GTP Loading, Kinases (MEK, Raf), p44 Mitogen-activated Protein Kinase, and c-fos Expression in Human*

Aortic Smooth Muscle Cells (∗). Journal of Biological Chemistry, 1996. **271**(18): p. 10660-10666.

87. Bhunia, A.K., et al., *Lactosylceramide Mediates Tumor Necrosis Factor-α-induced Intercellular Adhesion Molecule-1 (ICAM-1) Expression and the Adhesion of Neutrophil in Human Umbilical Vein Endothelial Cells* *. Journal of Biological Chemistry, 1998. **273**(51): p. 34349-34357.

88. Gong, N., et al., *Lactosylceramide recruits PKCα/ε and phospholipase A₂ to stimulate PECAM-1 expression in human monocytes and adhesion to endothelial cells.* Proceedings of the National Academy of Sciences of the United States of America, 2004. **101**(17): p. 6490-6495.

89. Martin, S.F., N. Williams, and S. Chatterjee, *Lactosylceramide is required in apoptosis induced by N-Smase.* Glycoconjugate Journal, 2006. **23**(3): p. 147-157.

90. Kolmakova, A., et al., *VEGF recruits lactosylceramide to induce endothelial cell adhesion molecule expression and angiogenesis in vitro and in vivo.* Glycoconjugate Journal, 2009. **26**(5): p. 547-558.

91. Schlingmann, K.P., W. Cassar, and M. Konrad, *Juvenile onset IIH and CYP24A1 mutations.* Bone Rep, 2018. **9**: p. 42-46.

92. Kaufmann, M., et al., *Clinical utility of simultaneous quantitation of 25-hydroxyvitamin D and 24, 25-dihydroxyvitamin D by LC-MS/MS involving derivatization with DMEQ-TAD.* The Journal of Clinical Endocrinology & Metabolism, 2014. **99**(7): p. 2567-2574.

93. Steiner, M., et al., *Comparison between Different Methods for Biomechanical Assessment of Ex Vivo Fracture Callus Stiffness in Small Animal Bone Healing Studies.* PloS one, 2015. **10**: p. e0119603.

94. Bosemark, P., H. Isaksson, and M. Tagil, *Influence of systemic bisphosphonate treatment on mechanical properties of BMP-induced calluses in a rat fracture model: comparison of three-point bending and twisting test.* J Orthop Res, 2014. **32**(5): p. 721-6.

APPENDIX

Copyrights and Permissions

- Figure 2
- Figure 7
- Figure 9
- Figure 24

Research Ethic Board Approval for Mice Studies

ELSEVIER LICENSE
TERMS AND CONDITIONS
Feb 16, 2022

This Agreement between Dr. Dila Kavame ("You") and Elsevier ("Elsevier") consists of your license details and the terms and conditions provided by Elsevier and Copyright Clearance Center.

License Number	5251131007105
License date	Feb 16, 2022
Licensed Content Publisher	Elsevier
Licensed Content Publication	Current Biology
Licensed Content Title	Endochondral ossification: A delicate balance between growth and mineralisation
Licensed Content Author	Alicia White,Gillian Wallis
Licensed Content Date	Aug 7, 2001
Licensed Content Volume	11
Licensed Content Issue	15
Licensed Content Pages	3
Start Page	R589
End Page	R591
Type of Use	reuse in a thesis/dissertation

Portion	figures/tables/illustrations
Number of figures/tables/illustrations	1
Format	electronic
Are you the author of this Elsevier article?	No
Will you be translating?	No
Title	Phenotyping an Idiopathic Infantile Hypercalcemia Mouse Model
Institution name	McGill University
Expected presentation date	Apr 2022
Portions	figure 1
Requestor Location	Dr. Dila Kavame 4084 Rue Clark Montreal, QC H2W1W9 Canada Attn: Dr. Dila Kavame
Publisher Tax ID	GB 494 6272 12
	0.00 USD
Total	

Terms and Conditions

INTRODUCTION

1. The publisher for this copyrighted material is Elsevier. By clicking "accept" in connection with completing this licensing transaction, you agree that the following terms and conditions apply to this transaction (along with the Billing and Payment terms and conditions established by Copyright Clearance Center, Inc. ("CCC"), at the time that you opened your Rightslink account and that are available at any time at http://myaccount.copyright.com).
GENERAL TERMS
Elsevier hereby grants you permission to reproduce the aforementioned material subject tothe terms and conditions indicated.
Acknowledgement: If any part of the material to be used (for example, figures) has appeared in our publication with credit or acknowledgement to another source, permission must also be sought from that source. If such permission is not obtained then that material may not be included in your publication/copies. Suitable acknowledgement to the source must be made, either as a footnote or in a reference list at the end of your publication, as follows:
"Reprinted from Publication title, Vol /edition number, Author(s), Title of article / title of chapter, Pages No., Copyright (Year), with permission from Elsevier [OR APPLICABLE SOCIETY COPYRIGHT OWNER]." Also Lancet special credit - "Reprinted from The Lancet, Vol. number, Author(s), Title of article, Pages No., Copyright (Year), with permission from Elsevier."
Reproduction of this material is confined to the purpose and/or media for which permission is hereby given.
Altering/Modifying Material: Not Permitted. However figures and illustrations may be altered/adapted minimally to serve your work. Any other abbreviations, additions, deletions and/or any other alterations shall be made only with prior written authorization of Elsevier Ltd. (Please contact Elsevier's permissions helpdesk here). No modifications can be made to any Lancet figures/tables and they must be reproduced in full.
If the permission fee for the requested use of our material is waived in this instance,please be advised that your future requests for Elsevier materials may attract a fee.
Reservation of Rights: Publisher reserves all rights not specifically granted in the combination of (i) the license details provided by you and accepted in the course of this licensing transaction, (ii) these terms and conditions and (iii) CCC's Billing and Payment terms and conditions.
License Contingent Upon Payment: While you may exercise the rights licensedimmediately upon issuance of the license at the end of the licensing process for the transaction, provided that you have disclosed complete and accurate details of your proposed use, no license is finally effective unless and until full payment is received from you (either by publisher or by CCC) as provided in CCC's Billing and Payment terms and conditions. If full payment is not received on a timely basis, then any license preliminarily granted shall be deemed automatically revoked and shall be void as if never granted. Further, in the event that you breach any of these terms and conditions or any of CCC's Billing and Payment terms and conditions, the license is automatically revoked and shall be void as if never granted. Use of materials as described in a revoked license, as well as any use of the materials beyond the scope of an unrevoked license, may constitute copyright infringement and publisher reserves the right to take any and all action to protect its copyright in the materials.
Warranties: Publisher makes no representations or warranties with respect to the licensedmaterial.
Indemnity: You hereby indemnify and agree to hold harmless publisher and CCC, andtheir respective officers, directors, employees and agents, from and against any and all claims arising

out of your use of the licensed material other than as specifically authorized pursuant to this license.
No Transfer of License: This license is personal to you and may not be sublicensed,assigned, or transferred by you to any other person without publisher's written permission.
No Amendment Except in Writing: This license may not be amended except in a writingsigned by both parties (or, in the case of publisher, by CCC on publisher's behalf).
Objection to Contrary Terms: Publisher hereby objects to any terms contained in anypurchase order, acknowledgment, check endorsement or other writing prepared by you, which terms are inconsistent with these terms and conditions or CCC's Billing and Payment terms and conditions. These terms and conditions, together with CCC's Billing and Payment terms and conditions (which are incorporated herein), comprise the entire agreement between you and publisher (and CCC) concerning this licensing transaction. In the event of any conflict between your obligations established by these terms and conditions and those established by CCC's Billing and Payment terms and conditions, these terms and conditions shall control.
Revocation: Elsevier or Copyright Clearance Center may deny the permissions describedin this License at their sole discretion, for any reason or no reason, with a full refund payable to you. Notice of such denial will be made using the contact information provided by you. Failure to receive such notice will not alter or invalidate the denial. In no event will Elsevier or Copyright Clearance Center be responsible or liable for any costs, expenses or damage incurred by you as a result of a denial of your permission request, other than a refund of the amount(s) paid by you to Elsevier and/or Copyright Clearance Center for denied permissions.
LIMITED LICENSE
The following terms and conditions apply only to specific license types:
Translation: This permission is granted for non-exclusive world **English** rights only unless your license was granted for translation rights. If you licensed translation rights you may only translate this content into the languages you requested. A professional translator must perform all translations and reproduce the content word for word preserving the integrity of the article.
Posting licensed content on any Website: The following terms and conditions apply as follows: Licensing material from an Elsevier journal: All content posted to the web site must maintain the copyright information line on the bottom of each image; A hyper-text must be included to the Homepage of the journal from which you are licensing at http://www.sciencedirect.com/science/journal/xxxxx or the Elsevier homepage for books at http://www.elsevier.com; Central Storage: This license does not include permission for a scanned version of the material to be stored in a central repository such as that provided by Heron/XanEdu.
Licensing material from an Elsevier book: A hyper-text link must be included to the Elsevier homepage at http://www.elsevier.com . All content posted to the web site must maintain the copyright information line on the bottom of each image.
Posting licensed content on Electronic reserve: In addition to the above the following clauses are applicable: The web site must be password-protected and made available only to bona fide students registered on a relevant course. This permission is granted for 1 year only. You may obtain a new license for future website posting.
For journal authors: the following clauses are applicable in addition to the above:
Preprints:

A preprint is an author's own write-up of research results and analysis, it has not been peerreviewed, nor has it had any other value added to it by a publisher (such as formatting, copyright, technical enhancement etc.).
Authors can share their preprints anywhere at any time. Preprints should not be added to or enhanced in any way in order to appear more like, or to substitute for, the final versions of articles however authors can update their preprints on arXiv or RePEc with their Accepted Author Manuscript (see below).
If accepted for publication, we encourage authors to link from the preprint to their formal publication via its DOI. Millions of researchers have access to the formal publications on ScienceDirect, and so links will help users to find, access, cite and use the best available version.
Please note that Cell Press, The Lancet and some society-owned have different preprint policies. Information on these policies is available on the journal homepage.
Accepted Author Manuscripts: An accepted author manuscript is the manuscript of an article that has been accepted for publication and which typically includes authorincorporated changes suggested during submission, peer review and editor-author communications.
Authors can share their accepted author manuscript:

- immediately via their non-commercial person homepage or blog
    - by updating a preprint in arXiv or RePEc with the accepted manuscript via their
    - research institute or institutional repository for internal institutional uses or as part
    - of an invitation-only research collaboration work-group directly by providing copies to their students or to research collaborators for their personal use
    - for private scholarly sharing as part of an invitation-only work group on commercial sites with which Elsevier has an agreement
- After the embargo period via non-commercial hosting platforms such as their institutional repository via commercial sites with which Elsevier has an agreement In all cases accepted manuscripts should:
    - link to the formal publication via its DOI bear a CC-BY-NC-ND license - this is easy to do
    - if aggregated with other manuscripts, for example in a repository or other site, be shared in
    - alignment with our hosting policy not be added to or enhanced in any way to appear more like, or to substitute for, the published journal article.

Published journal article (JPA): A published journal article (PJA) is the definitive final record of published research that appears or will appear in the journal and embodies all value-adding publishing activities including peer review co-ordination, copy-editing, formatting, (if relevant) pagination and online enrichment.
Policies for sharing publishing journal articles differ for subscription and gold open access articles:
Subscription Articles: If you are an author, please share a link to your article rather than the full-text. Millions of researchers have access to the formal publications on ScienceDirect, and so links will help your users to find, access, cite, and use the best available version.
Theses and dissertations which contain embedded PJAs as part of the formal submission can be posted publicly by the awarding institution with DOI links back to the formal publications on ScienceDirect.
If you are affiliated with a library that subscribes to ScienceDirect you have additional private sharing rights for others' research accessed under that agreement. This includes use for classroom teaching and internal training at the institution (including use in course packs and courseware programs), and inclusion of the article for grant funding purposes.

Gold Open Access Articles: May be shared according to the author-selected end-user license and should contain a CrossMark logo, the end user license, and a DOI link to the formal publication on ScienceDirect.
Please refer to Elsevier's posting policy for further information.
For book authors the following clauses are applicable in addition to the above: Authors are permitted to place a brief summary of their work online only. You are not allowed to download and post the published electronic version of your chapter, nor may you scan the printed edition to create an electronic version. **Posting to a repository:** Authors are permitted to post a summary of their chapter only in their institution's repository.
Thesis/Dissertation: If your license is for use in a thesis/dissertation your thesis may be submitted to your institution in either print or electronic form. Should your thesis be published commercially, please reapply for permission. These requirements include permission for the Library and Archives of Canada to supply single copies, on demand, of the complete thesis and include permission for Proquest/UMI to supply single copies, on demand, of the complete thesis. Should your thesis be published commercially, please reapply for permission. Theses and dissertations which contain embedded PJAs as part of the formal submission can be posted publicly by the awarding institution with DOI links back to the formal publications on ScienceDirect.

Elsevier Open Access Terms and Conditions
You can publish open access with Elsevier in hundreds of open access journals or in nearly 2000 established subscription journals that support open access publishing. Permitted third party re-use of these open access articles is defined by the author's choice of Creative Commons user license. See our open access license policy for more information.
Terms & Conditions applicable to all Open Access articles published with Elsevier:
Any reuse of the article must not represent the author as endorsing the adaptation of the article nor should the article be modified in such a way as to damage the author's honour or reputation. If any changes have been made, such changes must be clearly indicated.
The author(s) must be appropriately credited and we ask that you include the end user license and a DOI link to the formal publication on ScienceDirect.
If any part of the material to be used (for example, figures) has appeared in our publication with credit or acknowledgement to another source it is the responsibility of the user to ensure their reuse complies with the terms and conditions determined by the rights holder.
Additional Terms & Conditions applicable to each Creative Commons user license:
CC BY: The CC-BY license allows users to copy, to create extracts, abstracts and new works from the Article, to alter and revise the Article and to make commercial use of the Article (including reuse and/or resale of the Article by commercial entities), provided the user gives appropriate credit (with a link to the formal publication through the relevant DOI), provides a link to the license, indicates if changes were made and the licensor is not represented as endorsing the use made of the work. The full details of the license are available at http://creativecommons.org/licenses/by/4.0.
CC BY NC SA: The CC BY-NC-SA license allows users to copy, to create extracts, abstracts and new works from the Article, to alter and revise the Article, provided this is not done for commercial purposes, and that the user gives appropriate credit (with a link to the formal publication through the relevant DOI), provides a link to the license, indicates if changes were made and the licensor is not represented as endorsing the use made of the work. Further, any new

works must be made available on the same conditions. The full details of the license are available at http://creativecommons.org/licenses/by-nc-sa/4.0.
CC BY NC ND: The CC BY-NC-ND license allows users to copy and distribute the Article, provided this is not done for commercial purposes and further does not permit distribution of the Article if it is changed or edited in any way, and provided the user gives appropriate credit (with a link to the formal publication through the relevant DOI), provides a link to the license, and that the licensor is not represented as endorsing the use made of the work. The full details of the license are available at http://creativecommons.org/licenses/by-nc-nd/4.0. Any commercial reuse of Open Access articles published with a CC BY NC SA or CC BY NC ND license requires permission from Elsevier and will be subject to a fee.
Commercial reuse includes:

- Associating advertising with the full text of the Article
- Charging fees for document delivery or access
- Article aggregation
- Systematic distribution via e-mail lists or share buttons

Posting or linking by commercial companies for use by customers of those companies.

20. **Other Conditions**:

v1.10
Questions? customercare@copyright.com or +1-855-239-3415 (toll free in the US) or +1-978-646-2777.

SPRINGER NATURE LICENSE
TERMS AND CONDITIONS
Feb 16, 2022

This Agreement between Dr. Dila Kavame ("You") and Springer Nature ("Springer Nature") consists of your license details and the terms and conditions provided by Springer Nature and Copyright Clearance Center.

License Number	5251121060189
License date	Feb 16, 2022
Licensed Content Publisher	Springer Nature
Licensed Content Publication	Nature Reviews Rheumatology
Licensed Content Title	Fracture healing: mechanisms and interventions
Licensed Content Author	Thomas A. Einhorn et al
Licensed Content Date	Sep 30, 2014
Type of Use	Thesis/Dissertation
Requestor type	academic/university or research institute
Format	electronic
Portion	figures/tables/illustrations
Number of figures/tables/illustrations	1
High-res required	no
Will you be translating?	no

Circulation/distribution	1 - 29
Author of this Springer Nature content	no
Title	Phenotyping an Idiopathic Infantile Hypercalcemia Mouse Model
Institution name	McGill University
Expected presentation date	Apr 2022
Portions	Figure 2
Requestor Location	Dr. Dila Kavame 4084 Rue Clark Montreal, QC H2W1W9 Canada Attn: Dr. Dila Kavame
Total	0.00 CAD

Terms and Conditions

Springer Nature Customer Service Centre GmbH

Terms and Conditions

This agreement sets out the terms and conditions of the licence (the **Licence**) between you and **Springer Nature Customer Service Centre GmbH** (the **Licensor**). By clicking 'accept' and completing the transaction for the material (**Licensed Material**), you also confirm your acceptance of these terms and conditions.

Grant of License

1. 1. The Licensor grants you a personal, non-exclusive, non-transferable, world-wide licence to reproduce the Licensed Material for the purpose specified in your order only. Licences are granted for the specific use requested in the order and for no other use, subject to the conditions below.

1. 2. The Licensor warrants that it has, to the best of its knowledge, the rights to license reuse of the Licensed Material. However, you should ensure that the material you are requesting is original to the Licensor and does not carry the copyright of another entity (as credited in the published version).

1. 3. If the credit line on any part of the material you have requested indicates that it was reprinted or adapted with permission from another source, then you should also seek permission from that source to reuse the material.

Scope of Licence

2. 1. You may only use the Licensed Content in the manner and to the extent permitted by these Ts&Cs and any applicable laws.

2. 2. A separate licence may be required for any additional use of the Licensed Material, e.g. where a licence has been purchased for print only use, separate permission must be obtained for electronic re-use. Similarly, a licence is only valid in the language selected and does not apply for editions in other languages unless additional translation rights have been granted separately in the licence. Any content owned by third parties are expressly excluded from the licence.

2. 3. Similarly, rights for additional components such as custom editions and derivatives require additional permission and may be subject to an additional fee.

Please apply to Journalpermissions@springernature.com/bookpermissions@springernature.com for these rights.

2. 4. Where permission has been granted **free of charge** for material in print, permission may also be granted for any electronic version of that work, provided that the material is incidental to your work as a whole and that the electronic version is essentially equivalent to, or substitutes for, the print version.

2. 5. An alternative scope of licence may apply to signatories of the STM Permissions Guidelines, as amended from time to time.

Duration of Licence

3. 1. A licence for is valid from the date of purchase ('Licence Date') at the end of the relevant period in the below table:

Scope of		**Duration of Licence**	**Licence**
Books	Post on a website	12 months	and journals
Lifetime	Presentations	12 months	of the edition in
the			language
purchased			

Acknowledgement

4. 1. The Licensor's permission must be acknowledged next to the Licenced Material in print. In electronic form, this acknowledgement must be visible at the same time as the figures/tables/illustrations or abstract, and must be hyperlinked to the journal/book's homepage. Our required acknowledgement format is in the Appendix below.

Restrictions on use

5. 1. Use of the Licensed Material may be permitted for incidental promotional use and minor editing privileges e.g. minor adaptations of single figures, changes of format, colour and/or style where the adaptation is credited as set out in Appendix 1 below. Any other changes including but not limited to, cropping, adapting, omitting material that affect the meaning, intention or moral rights of the author are strictly prohibited.

5. 2. You must not use any Licensed Material as part of any design or trademark.

5. 3. Licensed Material may be used in Open Access Publications (OAP) before publication by Springer Nature, but any Licensed Material must be removed from OAP sites prior to final publication.

Ownership of Rights

6. 1. Licensed Material remains the property of either Licensor or the relevant third party and any rights not explicitly granted herein are expressly reserved.
Warranty
IN NO EVENT SHALL LICENSOR BE LIABLE TO YOU OR ANY OTHER PARTY OR ANY OTHER PERSON OR FOR ANY SPECIAL, CONSEQUENTIAL, INCIDENTAL OR INDIRECT DAMAGES, HOWEVER CAUSED, ARISING OUT OF OR IN CONNECTION WITH THE DOWNLOADING, VIEWING OR USE OF THE MATERIALS REGARDLESS OF THE FORM OF ACTION, WHETHER FOR BREACH OF CONTRACT, BREACH OF WARRANTY, TORT, NEGLIGENCE, INFRINGEMENT OR OTHERWISE (INCLUDING, WITHOUT LIMITATION, DAMAGES BASED ON LOSS OF PROFITS, DATA, FILES, USE, BUSINESS OPPORTUNITY OR CLAIMS OF THIRD PARTIES), AND
WHETHER OR NOT THE PARTY HAS BEEN ADVISED OF THE POSSIBILITY OF SUCH DAMAGES. THIS LIMITATION SHALL APPLY NOTWITHSTANDING ANY FAILURE OF ESSENTIAL PURPOSE OF ANY LIMITED REMEDY PROVIDED HEREIN.
Limitations
8. 1. ***BOOKS ONLY:***Where **'reuse in a dissertation/thesis'** has been selected the following terms apply: Print rights of the final author's accepted manuscript (for clarity, NOT the published version) for up to 100 copies, electronic rights for use only on a personal website or institutional repository as defined by the Sherpa guideline (www.sherpa.ac.uk/romeo/).
8. 2. For content reuse requests that qualify for permission under the STM Permissions Guidelines, which may be updated from time to time, the STM Permissions Guidelines supersede the terms and conditions contained in this licence.
Termination and Cancellation
9. 1. Licences will expire after the period shown in Clause 3 (above).
9. 2. Licensee reserves the right to terminate the Licence in the event that payment is not received in full or if there has been a breach of this agreement by you.
Appendix 1 — Acknowledgements:
For Journal Content:
Reprinted by permission from [**the Licensor**]: [**Journal Publisher** (e.g. Nature/Springer/Palgrave)] [**JOURNAL NAME**] [**REFERENCE CITATION** (Article name, Author(s) Name), [**COPYRIGHT**] (year of publication)
For **Advance Online Publication papers:**
Reprinted by permission from [**the Licensor**]: [**Journal Publisher** (e.g. Nature/Springer/Palgrave)] [**JOURNAL NAME**] [**REFERENCE CITATION** (Article name, Author(s) Name), [**COPYRIGHT**] (year of publication), advance online publication, day month year (doi: 10.1038/sj.[JOURNAL ACRONYM].)
For Adaptations/Translations:
Adapted/Translated by permission from [**the Licensor**]: [**Journal Publisher** (e.g. Nature/Springer/Palgrave)] [**JOURNAL NAME**] [**REFERENCE CITATION** (Article name, Author(s) Name), [**COPYRIGHT**] (year of publication)
Note: For any republication from the British Journal of Cancer, the following credit line style applies:
Reprinted/adapted/translated by permission from [**the Licensor**]: on behalf of Cancer Research UK: : [**Journal Publisher** (e.g. Nature/Springer/Palgrave)] [**JOURNAL**

NAME] [**REFERENCE CITATION** (Article name, Author(s) Name), [**COPYRIGHT]** (year of publication)
For **Advance Online Publication** papers:
Reprinted by permission from The [**the Licensor**]: on behalf of Cancer Research UK: [**Journal Publisher** (e.g. Nature/Springer/Palgrave)] [**JOURNAL NAME**] [**REFERENCE CITATION** (Article name, Author(s) Name), [**COPYRIGHT**] (year of publication), advance online publication, day month year (doi: 10.1038/sj. [JOURNAL ACRONYM])
For Book content:
Reprinted/adapted by permission from [**the Licensor**]: [**Book Publisher** (e.g. Palgrave Macmillan, Springer etc) [**Book Title**] by [**Book author**(s)] [**COPYRIGHT**] (year of publication) **Other Conditions**:
Version 1.3
Questions? customercare@copyright.com or +1-855-239-3415 (toll free in the US) or +1-978-646-2777.

SPRINGER NATURE LICENSE
TERMS AND CONDITIONS
Feb 17, 2022

This Agreement between Dr. Dila Kavame ("You") and Springer Nature ("Springer Nature") consists of your license details and the terms and conditions provided by Springer Nature and Copyright Clearance Center.

License Number	5251480172796
License date	Feb 17, 2022
Licensed Content Publisher	Springer Nature
Licensed Content Publication	Nature Reviews Cancer
Licensed Content Title	Vitamin D signalling pathways in cancer: potential for anticancer therapeutics
Licensed Content Author	Kristin K. Deeb et al
Licensed Content Date	Dec 31, 1969
Type of Use	Thesis/Dissertation
Requestor type	academic/university or research institute
Format	electronic
Portion	figures/tables/illustrations
Number of figures/tables/illustrations	1
Will you be translating?	no

Circulation/distribution	1 - 29
Author of this Springer Nature content	no
Title	Phenotyping an Idiopathic Infantile Hypercalcemia Mouse Model
Institution name	McGill University
Expected presentation date	Apr 2022
Portions	figure 1
Requestor Location	Dr. Dila Kavame 4084 Rue Clark Montreal, QC H2W1W9 Canada Attn: Dr. Dila Kavame
Total	0.00 USD

Terms and Conditions

Springer Nature Customer Service Centre GmbH

Terms and Conditions

This agreement sets out the terms and conditions of the licence (the **Licence**) between you and **Springer Nature Customer Service Centre GmbH** (the **Licensor**). By clicking 'accept' and completing the transaction for the material (**Licensed Material**), you also confirm your acceptance of these terms and conditions.

Grant of License

1. 1. The Licensor grants you a personal, non-exclusive, non-transferable, world-wide licence to reproduce the Licensed Material for the purpose specified in your order only. Licences are granted for the specific use requested in the order and for no other use, subject to the conditions below.

1. 2. The Licensor warrants that it has, to the best of its knowledge, the rights to license reuse of the Licensed Material. However, you should ensure that the material you are requesting is original to the Licensor and does not carry the copyright of another entity (as credited in the published version).

1. 3. If the credit line on any part of the material you have requested indicates that it was reprinted or adapted with permission from another source, then you should also seek permission from that source to reuse the material.

Scope of Licence

2. 1. You may only use the Licensed Content in the manner and to the extent permitted by these Ts&Cs and any applicable laws.

2. 2. A separate licence may be required for any additional use of the Licensed Material, e.g. where a licence has been purchased for print only use, separate permission must be obtained for electronic re-use. Similarly, a licence is only valid in the language selected and does not apply for editions in other languages unless additional translation rights have been granted separately in the licence. Any content owned by third parties are expressly excluded from the licence.

2. 3. Similarly, rights for additional components such as custom editions and derivatives require additional permission and may be subject to an additional fee.

Please apply to Journalpermissions@springernature.com/bookpermissions@springernature.com for these rights.

2. 4. Where permission has been granted **free of charge** for material in print, permission may also be granted for any electronic version of that work, provided that the material is incidental to your work as a whole and that the electronic version is essentially equivalent to, or substitutes for, the print version.

2. 5. An alternative scope of licence may apply to signatories of the STM Permissions Guidelines, as amended from time to time.

Duration of Licence

3. 1. A licence for is valid from the date of purchase ('Licence Date') at the end of the relevant period in the below table:

Scope of		**Duration of Licence**	**Licence**
Books	Post on a website	12 months	and journals
Lifetime	Presentations	12 months	of the edition in
the			language
purchased			

Acknowledgement

4. 1. The Licensor's permission must be acknowledged next to the Licenced Material in print. In electronic form, this acknowledgement must be visible at the same time as the figures/tables/illustrations or abstract, and must be hyperlinked to the journal/book's homepage. Our required acknowledgement format is in the Appendix below.

Restrictions on use

5. 1. Use of the Licensed Material may be permitted for incidental promotional use and minor editing privileges e.g. minor adaptations of single figures, changes of format, colour and/or style where the adaptation is credited as set out in Appendix 1 below. Any other changes including but not limited to, cropping, adapting, omitting material that affect the meaning, intention or moral rights of the author are strictly prohibited.

5. 2. You must not use any Licensed Material as part of any design or trademark.

5. 3. Licensed Material may be used in Open Access Publications (OAP) before publication by Springer Nature, but any Licensed Material must be removed from OAP sites prior to final publication.

Ownership of Rights

6. 1. Licensed Material remains the property of either Licensor or the relevant third party and any rights not explicitly granted herein are expressly reserved.

Warranty

IN NO EVENT SHALL LICENSOR BE LIABLE TO YOU OR ANY OTHER PARTY OR ANY OTHER PERSON OR FOR ANY SPECIAL, CONSEQUENTIAL, INCIDENTAL OR INDIRECT DAMAGES, HOWEVER CAUSED, ARISING OUT OF OR IN CONNECTION WITH THE DOWNLOADING, VIEWING OR USE OF THE MATERIALS REGARDLESS OF THE FORM OF ACTION, WHETHER FOR BREACH OF CONTRACT, BREACH OF WARRANTY, TORT, NEGLIGENCE, INFRINGEMENT OR OTHERWISE (INCLUDING, WITHOUT LIMITATION, DAMAGES BASED ON LOSS OF PROFITS, DATA, FILES, USE, BUSINESS OPPORTUNITY OR CLAIMS OF THIRD PARTIES), AND

WHETHER OR NOT THE PARTY HAS BEEN ADVISED OF THE POSSIBILITY OF SUCH DAMAGES. THIS LIMITATION SHALL APPLY NOTWITHSTANDING ANY FAILURE OF ESSENTIAL PURPOSE OF ANY LIMITED REMEDY PROVIDED HEREIN.

Limitations

8. 1. ***BOOKS ONLY:*** Where **'reuse in a dissertation/thesis'** has been selected the following terms apply: Print rights of the final author's accepted manuscript (for clarity, NOT the published version) for up to 100 copies, electronic rights for use only on a personal website or institutional repository as defined by the Sherpa guideline (www.sherpa.ac.uk/romeo/).

8. 2. For content reuse requests that qualify for permission under the STM Permissions Guidelines, which may be updated from time to time, the STM Permissions Guidelines supersede the terms and conditions contained in this licence.

Termination and Cancellation

9. 1. Licences will expire after the period shown in Clause 3 (above).

9. 2. Licensee reserves the right to terminate the Licence in the event that payment is not received in full or if there has been a breach of this agreement by you.

Appendix 1 — Acknowledgements:

For Journal Content:

Reprinted by permission from [**the Licensor**]: [**Journal Publisher** (e.g. Nature/Springer/Palgrave)] [**JOURNAL NAME**] [**REFERENCE CITATION** (Article name, Author(s) Name), [**COPYRIGHT**] (year of publication)

For **Advance Online Publication papers:**

Reprinted by permission from [**the Licensor**]: [**Journal Publisher** (e.g. Nature/Springer/Palgrave)] [**JOURNAL NAME**] [**REFERENCE CITATION** (Article name, Author(s) Name), [**COPYRIGHT**] (year of publication), advance online publication, day month year (doi: 10.1038/sj.[JOURNAL ACRONYM].)

For Adaptations/Translations:

Adapted/Translated by permission from [**the Licensor**]: [**Journal Publisher** (e.g. Nature/Springer/Palgrave)] [**JOURNAL NAME**] [**REFERENCE CITATION** (Article name, Author(s) Name), [**COPYRIGHT**] (year of publication)

Note: For any republication from the British Journal of Cancer, the following credit line style applies:

Reprinted/adapted/translated by permission from [**the Licensor**]: on behalf of Cancer Research UK: : [**Journal Publisher** (e.g. Nature/Springer/Palgrave)] [**JOURNAL**

NAME] [**REFERENCE CITATION** (Article name, Author(s) Name), [**COPYRIGHT]** (year of publication)
For **Advance Online Publication** papers:
Reprinted by permission from The [**the Licensor**]: on behalf of Cancer Research UK: [**Journal Publisher** (e.g. Nature/Springer/Palgrave)] [**JOURNAL NAME**] [**REFERENCE CITATION** (Article name, Author(s) Name), [**COPYRIGHT**] (year of publication), advance online publication, day month year (doi: 10.1038/sj. [JOURNAL ACRONYM])
For Book content:
Reprinted/adapted by permission from [**the Licensor**]: [**Book Publisher** (e.g. Palgrave Macmillan, Springer etc) [**Book Title**] by [**Book author**(s)] [**COPYRIGHT**] (year of publication) **Other Conditions**:
Version 1.3
Questions? customercare@copyright.com or +1-855-239-3415 (toll free in the US) or +1-978-646-2777.

JOHN WILEY AND SONS LICENSE
TERMS AND CONDITIONS
Feb 28, 2022

This Agreement between Dr. Dila Kavame ("You") and John Wiley and Sons ("John Wiley and Sons") consists of your license details and the terms and conditions provided by John Wiley and Sons and Copyright Clearance Center.

License Number	5257540444400		
Licensed Content Pages	6	License date	Feb 28, 2022
Type of use	Dissertation/Thesis	Licensed Content Publisher	John Wiley and Sons
Requestor type	University/Academic	Licensed Content Publication	Journal of Orthopaedic Research
Format	Print	Licensed Content Title	InBMPfluence of systemic bisphosphonate treatment on mechanical properties ofinduced calluses in a rat fracture model: Comparison of three point bending and twisting test
Portion	Figure/table	Licensed Content Author	Per Bosemark, Hanna Isaksson, Magnus Tägil
Number of Issue figures/tables	1	Licensed Content Date	Feb 13, 2014
Will you be translating?	No	Licensed Content Volume	32
		Licensed Content	5

Title	Phenotyping an Idiopathic Infantile Hypercalcemia Mouse Model
Institution name	McGill University
Expected presentation date	Apr 2022

Portions	figure 2
Requestor Location	Dr. Dila Kavame 4084 Rue Clark Montreal, QC H2W1W9 Canada Attn: Dr. Dila Kavame
Publisher Tax ID	EU826007151
Total	0.00 USD

Terms and Conditions

TERMS AND CONDITIONS

This copyrighted material is owned by or exclusively licensed to John Wiley & Sons, Inc. or one of its group companies (each a"Wiley Company") or handled on behalf of a society with which a Wiley Company has exclusive publishing rights in relation to a particular work (collectively "WILEY"). By clicking "accept" in connection with completing this licensing transaction, you agree that the following terms and conditions apply to this transaction (along with the billing and payment terms and conditions established by the Copyright Clearance Center Inc., ("CCC's Billing and Payment terms and conditions"), at the time that you opened your RightsLink account (these are available at any time at http://myaccount.copyright.com).

Terms and Conditions

- The materials you have requested permission to reproduce or reuse (the "Wiley Materials") are protected by copyright.
- You are hereby granted a personal, non-exclusive, non-sub licensable (on a standalone basis), non-transferable, worldwide, limited license to reproduce the Wiley Materials for the purpose specified in the licensing process. This license, **and any CONTENT (PDF or image file) purchased as part of your order,** is for a one-time use only and limited to any maximum distribution number specified in the license. The first instance of republication or reuse granted by this license must be completed within two years of the date of the grant of this license (although copies prepared before the end date may be distributed thereafter). The Wiley Materials shall not be used in any other manner or for any other purpose, beyond what is granted in the license. Permission is granted subject to an appropriate acknowledgement given to the author, title of the material/book/journal and the publisher. You shall also duplicate the copyright notice that appears in the Wiley publication in your use of the Wiley Material. Permission is also granted on the understanding that nowhere in the text is a previously published source acknowledged for all or part of this Wiley Material. Any third party content is expressly excluded from this permission.
- With respect to the Wiley Materials, all rights are reserved. Except as expressly granted by the terms of the license, no part of the Wiley Materials may be copied, modified, adapted (except for minor reformatting required by the new Publication), translated, reproduced, transferred or distributed, in any form or by any means, and no derivative works may be made based on the

Wiley Materials without the prior permission of the respective copyright owner.**For STM Signatory Publishers clearing permission under the terms of the STM Permissions Guidelines only, the terms of the license are extended to include subsequent editions and for editions in other languages, provided such editions are for the work as a whole in situ and does not involve the separate exploitation of the permitted figures or extracts,** You may not alter, remove or suppress in any manner any copyright, trademark or other notices displayed by the Wiley Materials. You may not license, rent, sell, loan, lease, pledge, offer as security, transfer or assign the Wiley Materials on a stand-alone basis, or any of the rights granted to you hereunder to any other person.

- The Wiley Materials and all of the intellectual property rights therein shall at all times remain the exclusive property of John Wiley & Sons Inc, the Wiley Companies, or their respective licensors, and your interest therein is only that of having possession of and the right to reproduce the Wiley Materials pursuant to Section 2 herein during the continuance of this Agreement. You agree that you own no right, title or interest in or to the Wiley Materials or any of the intellectual property rights therein. You shall have no rights hereunder other than the license as provided for above in Section 2. No right, license or interest to any trademark, trade name, service mark or other branding ("Marks") of WILEY or its licensors is granted hereunder, and you agree that you shall not assert any such right, license or interest with respect thereto
- NEITHER WILEY NOR ITS LICENSORS MAKES ANY WARRANTY OR REPRESENTATION OF ANY KIND TO YOU OR ANY THIRD PARTY, EXPRESS, IMPLIED OR STATUTORY, WITH RESPECT TO THE MATERIALS OR THE ACCURACY OF ANY INFORMATION CONTAINED IN THE MATERIALS, INCLUDING, WITHOUT LIMITATION, ANY IMPLIED WARRANTY OF MERCHANTABILITY, ACCURACY, SATISFACTORY QUALITY, FITNESS FOR A PARTICULAR PURPOSE, USABILITY, INTEGRATION OR NON-INFRINGEMENT AND ALL SUCH WARRANTIES ARE HEREBY EXCLUDED BY WILEY AND ITS LICENSORS AND WAIVED BY YOU.
- WILEY shall have the right to terminate this Agreement immediately upon breach of this Agreement by you.
- You shall indemnify, defend and hold harmless WILEY, its Licensors and their respective directors, officers, agents and employees, from and against any actual or threatened claims, demands, causes of action or proceedings arising from any breach of this Agreement by you.
- IN NO EVENT SHALL WILEY OR ITS LICENSORS BE LIABLE TO YOU OR ANY OTHER PARTY OR ANY OTHER PERSON OR ENTITY FOR ANY SPECIAL, CONSEQUENTIAL, INCIDENTAL, INDIRECT, EXEMPLARY OR PUNITIVE DAMAGES, HOWEVER CAUSED, ARISING OUT OF OR IN CONNECTION WITH THE DOWNLOADING, PROVISIONING, VIEWING OR USE OF THE MATERIALS REGARDLESS OF THE FORM OF ACTION, WHETHER FOR BREACH OF CONTRACT, BREACH OF WARRANTY, TORT, NEGLIGENCE, INFRINGEMENT OR OTHERWISE (INCLUDING, WITHOUT LIMITATION, DAMAGES BASED ON LOSS OF PROFITS, DATA, FILES, USE, BUSINESS OPPORTUNITY OR CLAIMS OF THIRD PARTIES), AND WHETHER OR NOT THE PARTY HAS BEEN ADVISED OF THE POSSIBILITY OF SUCH DAMAGES. THIS LIMITATION SHALL APPLY NOTWITHSTANDING ANY FAILURE OF ESSENTIAL PURPOSE OF ANY LIMITED REMEDY PROVIDED HEREIN.

- Should any provision of this Agreement be held by a court of competent jurisdiction to be illegal, invalid, or unenforceable, that provision shall be deemed amended to achieve as nearly as possible the same economic effect as the original provision, and the legality, validity and enforceability of the remaining provisions of this Agreement shall not be affected or impaired thereby.
- The failure of either party to enforce any term or condition of this Agreement shall not constitute a waiver of either party's right to enforce each and every term and condition of this Agreement. No breach under this agreement shall be deemed waived or excused by either party unless such waiver or consent is in writing signed by the party granting such waiver or consent. The waiver by or consent of a party to a breach of any provision of this Agreement shall not operate or be construed as a waiver of or consent to any other or subsequent breach by such other party.
- This Agreement may not be assigned (including by operation of law or otherwise) by you without WILEY's prior written consent.
- Any fee required for this permission shall be non-refundable after thirty (30) days from receipt by the CCC.
- These terms and conditions together with CCC's Billing and Payment terms and conditions (which are incorporated herein) form the entire agreement between you and WILEY concerning this licensing transaction and (in the absence of fraud) supersedes all prior agreements and representations of the parties, oral or written. This Agreement may not be amended except in writing signed by both parties. This Agreement shall be binding upon and inure to the benefit of the parties' successors, legal representatives, and authorized assigns.
- In the event of any conflict between your obligations established by these terms and conditions and those established by CCC's Billing and Payment terms and conditions, these terms and conditions shall prevail.
- WILEY expressly reserves all rights not specifically granted in the combination of (i) the license details provided by you and accepted in the course of this licensing transaction, (ii) these terms and conditions and (iii) CCC's Billing and Payment terms and conditions.
- This Agreement will be void if the Type of Use, Format, Circulation, or Requestor Type was misrepresented during the licensing process.
- This Agreement shall be governed by and construed in accordance with the laws of the State of New York, USA, without regards to such state's conflict of law rules. Any legal action, suit or proceeding arising out of or relating to these Terms and Conditions or the breach thereof shall be instituted in a court of competent jurisdiction in New York County in the State of New York in the United States of America and each party hereby consents and submits to the personal jurisdiction of such court, waives any objection to venue in such court and consents to service of process by registered or certified mail, return receipt requested, at the last known address of such party.

WILEY OPEN ACCESS TERMS AND CONDITIONS

Wiley Publishes Open Access Articles in fully Open Access Journals and in Subscription journals offering Online Open. Although most of the fully Open Access journals publish open access articles under the terms of the Creative Commons Attribution (CC BY) License only, the subscription journals and a few of the Open Access Journals offer a choice of Creative Commons Licenses. The license type is clearly identified on the article.

The Creative Commons Attribution License

McGill

July 20, 2021

Animal Certificate

This is to certify that **Dr. Rene St-Arnaud, Department of Medicine, Shriners Hospital,** currently holds an approved **Animal Use Protocol # 2001-4138** with McGill University and its Affiliated Hospital's Research Institutes for the following project:

Animal Use Protocol Title: Optimal bone fracture repair requires 24,25-dihydroxyvitamin D and its effector molecule, FAM57B2

Start date: July 1, 2021

Expiration date: June 30, 2022

McGill University and Affiliated Hospitals Research Institutes recognize the importance of animal research in our efforts to further our knowledge of natural processes, diseases and conservation. Research, educational and testing projects are conducted with full commitment to the wellbeing of the animal subjects. In order to limit animal use to meritorious research or educational projects, the institution relies on stringent peer review processes, along with assessment of ethical issues by the Animal Care Committee. McGill University recognizes that the use of animals in research, teaching and testing carries significant responsibilities. The institution will continue to develop and maintain guidelines and regulations, following the high standards established by the Canadian Council on Animal Care. It is committed to conducting the highest-quality research and to providing animals with the best care.

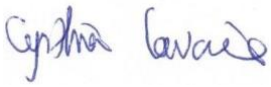

Cynthia Lavoie
Animal Ethics and Compliance Administrator
Animal Compliance Office
Office of Vice-Principal (Research and Innovation)
Suite 325, James Administration Building, McGill University
845 Sherbrooke Street West, Montreal, Quebec, Canada H3A 0G4
animal.approvals@mcgill.ca